Surface-Initiated Polymerization & Polymer Brushes

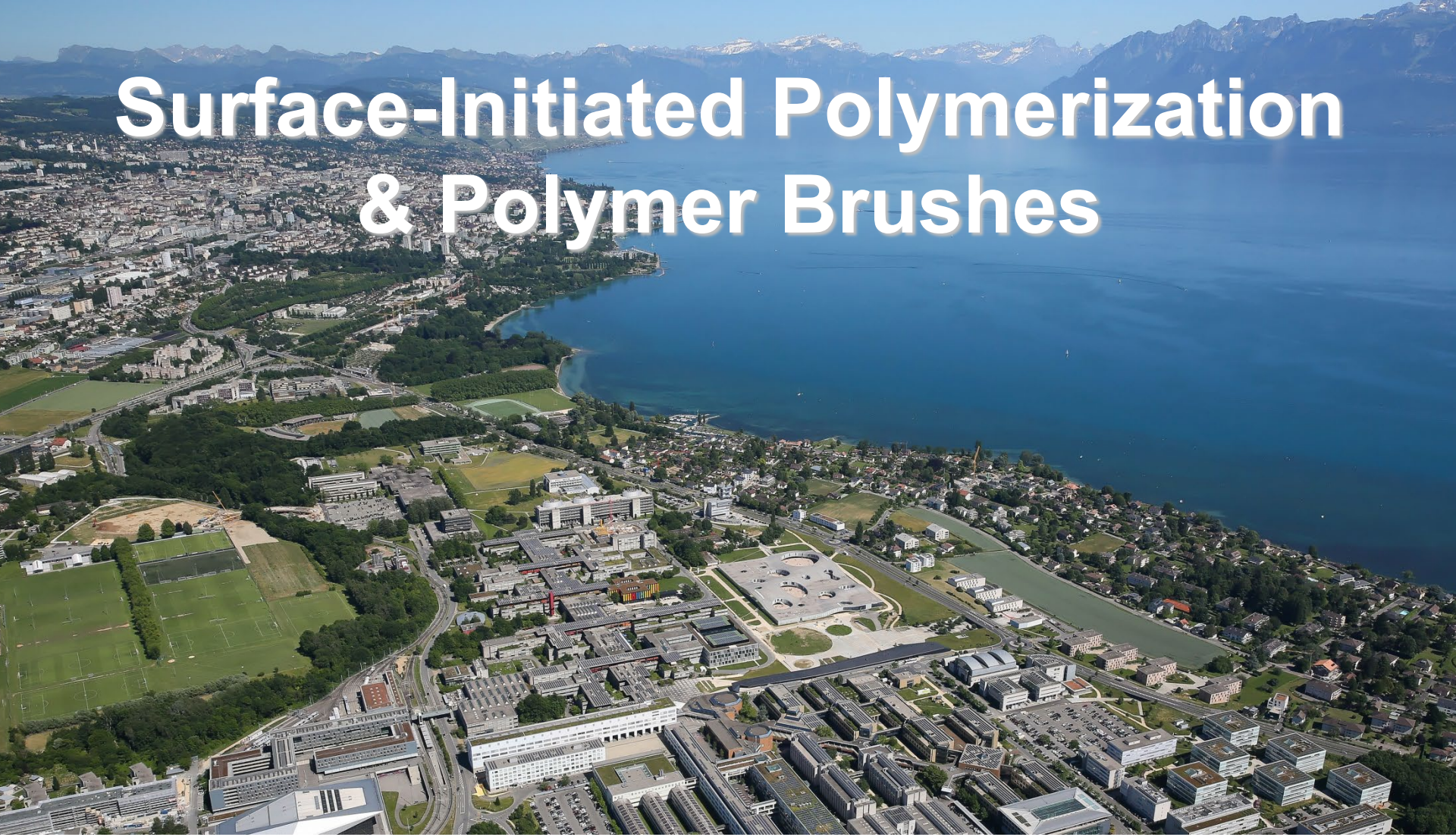

POLYMERS LABORATORY
LABORATOIRE DES POLYMÈRES

harm-anton.klok@epfl.ch

https://lp.epfl.ch/

@KlokLab

EPFL

What is a polymer brush (and when is a brush a brush….)?

Making polymer brushes

Characterizing polymer brushes

What are polymer brushes good for ?

Brushes

Molecular Brushes

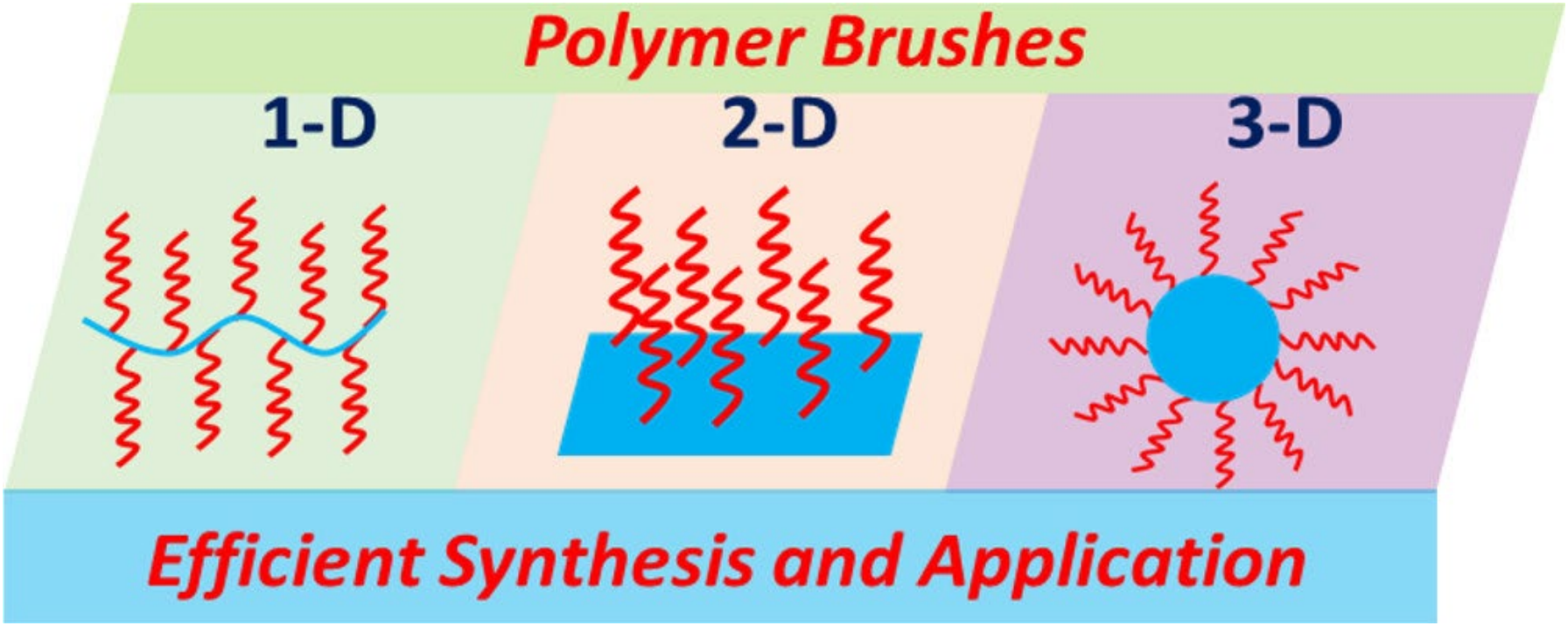

C. Feng, X. Huang, *Acc. Chem. Res.* **2018**, *51*, 2314–2323

What are Polymer Brushes ?

For this lecture and today, polymer brushes are assemblies of polymers that are tethered via one chain end to a solid (planar or spherical) substrate

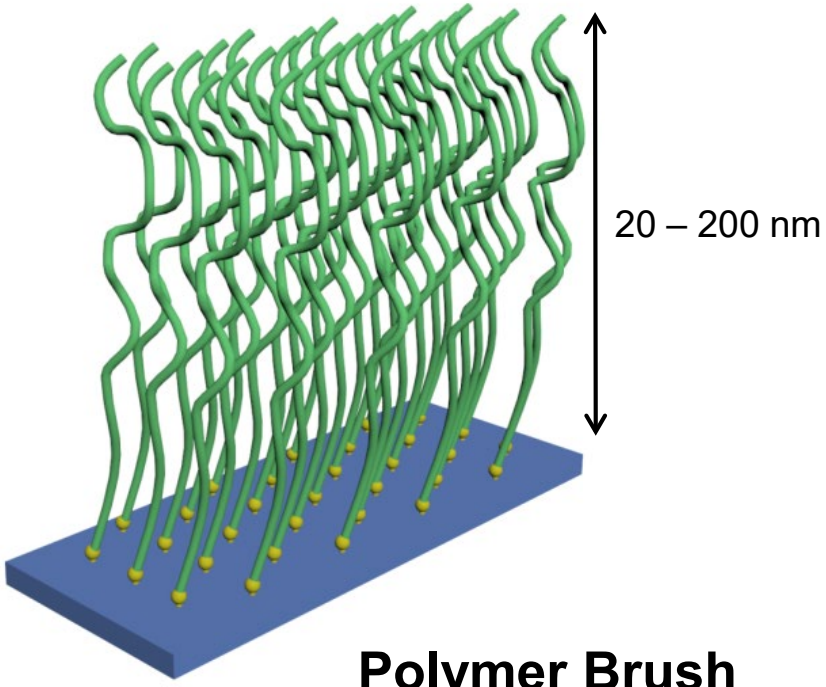

Polymer Brush

Main Structural Parameters of Polymer Brushes

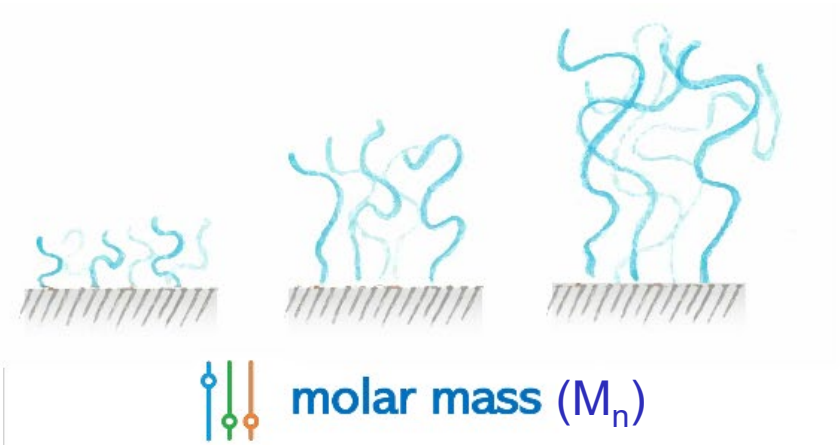

molar mass (M_n)

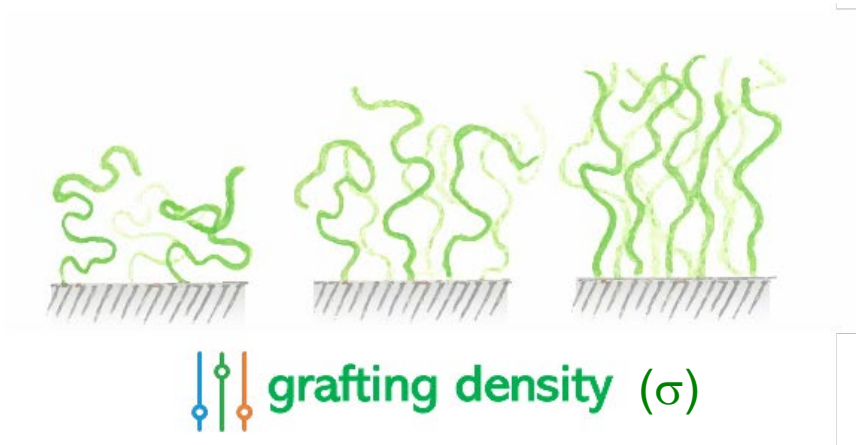

grafting density (σ)

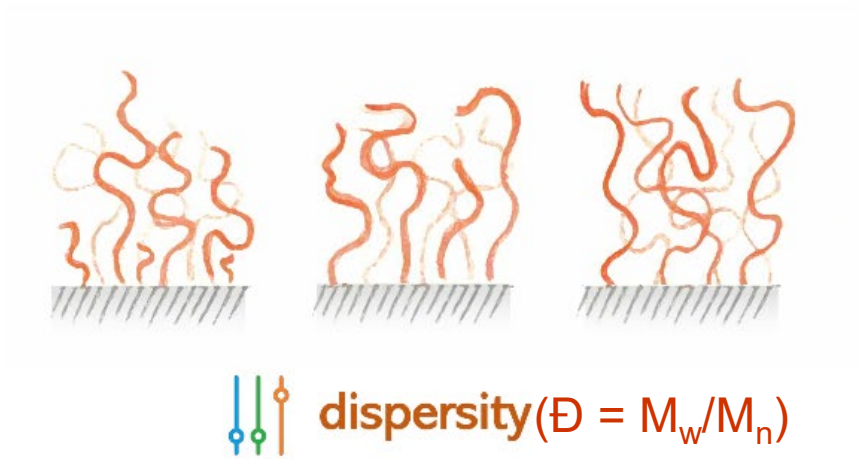

dispersity ($Đ = M_w/M_n$)

Note: molar mass and grafting density are directly related to the dry film thickness of a polymer brush:

- At a given grafting density, changing polymer molecular weight will result in a change in dry film thickness
- For a given polymer molecular weight, changing the grafting density will lead to a change in film thickness

Image credit: Prof. E. Benetti (Padua)

When is a Brush a Brush ?

Grafting density (nm^{-2}):

$$\sigma = \frac{h\,\rho\,NA}{M_n}$$

h: dry film thickness of the brush
ρ : polymer density
$N_{A:}$ Avogadro's constant
M_n: number-average molecular weight of the polymer grafts

Reduced tethering density:

$$\Sigma = \sigma\,\pi\,Rg^2$$

R_g : radius of gyration of a tethered chain at specific experimental conditions of solvent and temperature

Σ represents the number of chains that occupy the surface area covered by a single chain under ideal conditions

the highly stretched "brush regime" ($\Sigma \gg 1$)

the "crossover regime" ($\Sigma \approx 1$)

the "mushroom" or weakly interacting regime ($\Sigma < 1$)

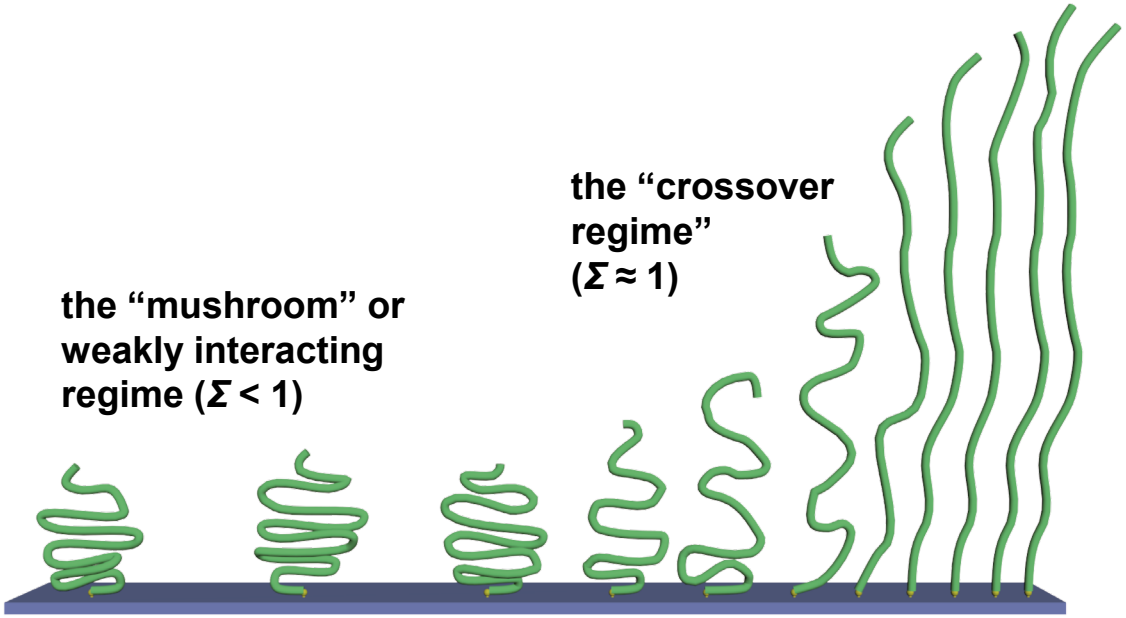

Conformations of Chain-end Tethered Polymers

The conformation of surface-anchored polymer chains is determined by

(i) The grafting density

(ii) Polymer - substrate, polymer – polymer, and polymer – solvent interactions

(iii) pH, temperature, ionic strength

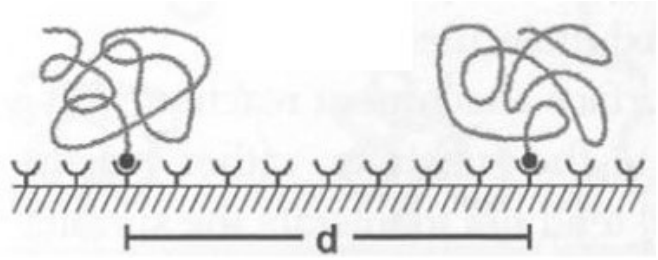

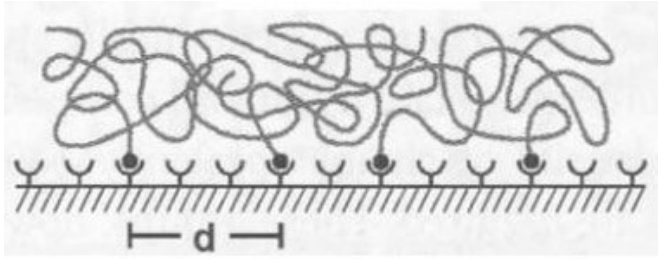

If the distance between two anchoring points is larger than the radius of gyration of the polymer chains, they act as single chains (no specific steric hindrance).

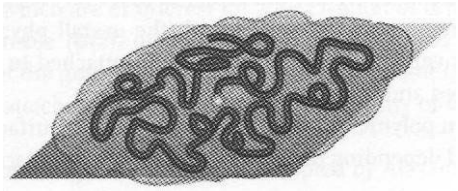

Pancake conformation

(strong interaction between the chains and the surface)

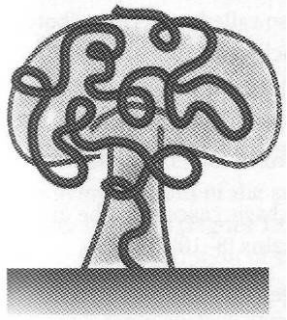

Mushroom conformation

(weak interaction between the chains and the surface)

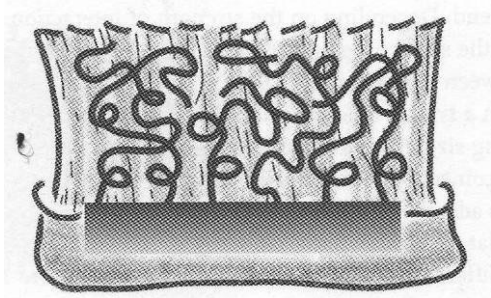

Rühe, J. in: *Polymer Brushes* (Advincula, R. C., Brittain, W. J., Caster, K. C., Ruhe, J., Eds.) WILEY-VCH, Weinheim, **2004**.

What is a polymer brush (and when is a brush a brush….)?

Making polymer brushes

Characterizing polymer brushes

What are polymer brushes good for ?

Polymer Brushes

Grafting onto:

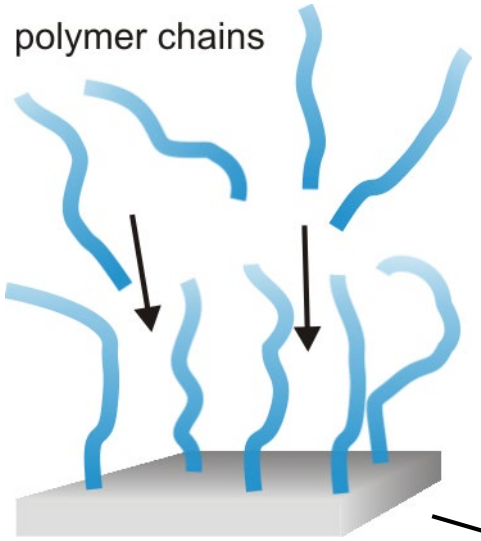

- Experimentally simple
- Limited grafting densities
- Limited film thicknesses

Grafting from:

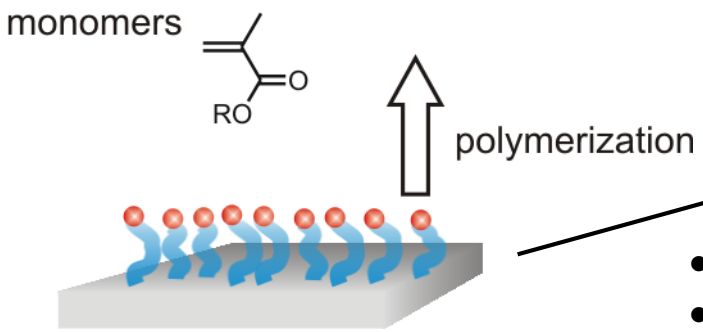

- Multistep protocol
- High grafting densities
- Control over film thickness and composition

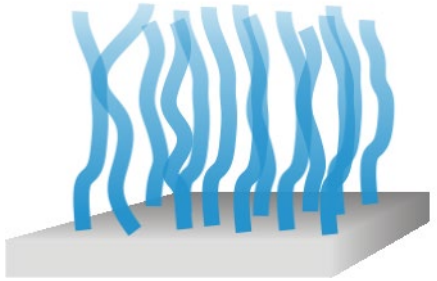

- High surface concentration of functional groups
- 3D substrates

R. Barbey, L. Lavanant, D. Paripovic, N. Schüwer, C. Sugnaux, S. Tugulu, H.-A. Klok, *Chem. Rev.* **2009**, *109*, 5437

Surface-Initiated Polymerization (SIP)

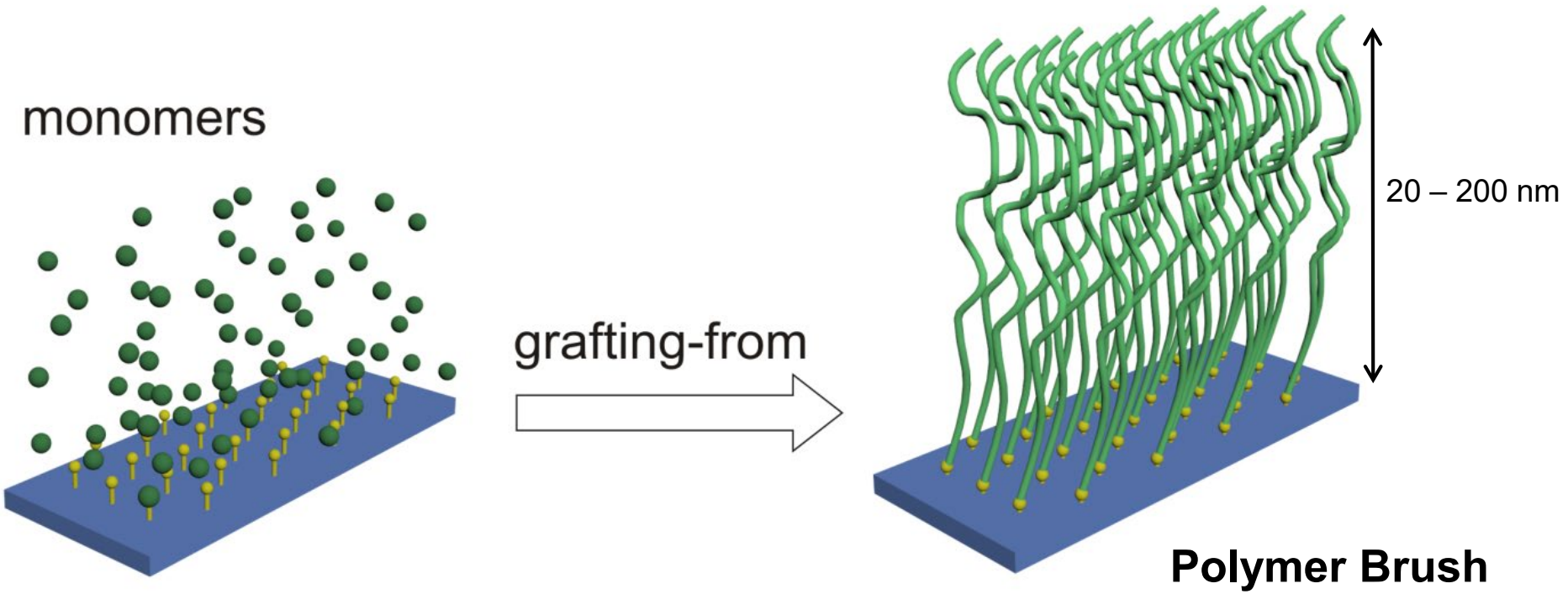

R. Barbey, L. Lavanant, D. Paripovic, N. Schüwer, C. Sugnaux, S. Tugulu, H.-A. Klok, *Chem. Rev.* **2009**, *109*, 5437
J. Zoppe, N. Cavusoglu Ataman, P. Mocny, J. Wang, J. Moraes, H.-A. Klok, *Chem. Rev.* **2017**, *117*, 1105

Surface-Initiated Polymerization (SIP)

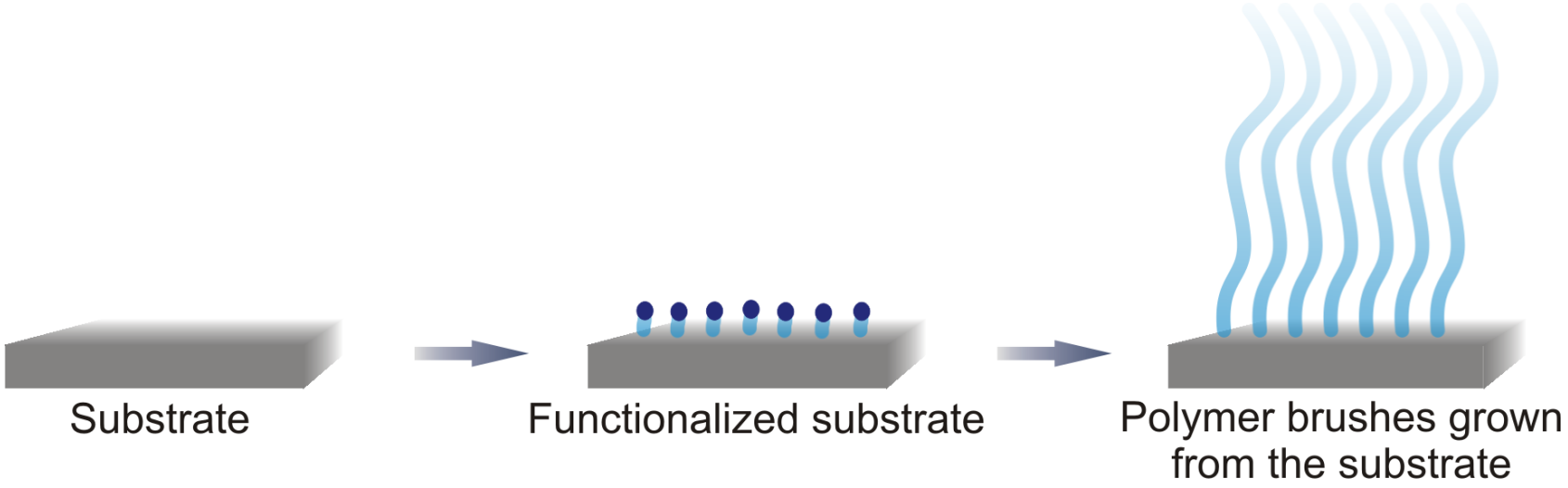

With the appropriate surface chemistry, brushes can be grown from "any" substrate

Surface-initiated controlled / "living" polymerizations allow:

- High grafting densities (fast and quantitative initiation)
- Control over film thickness via polymerization time
- Access to a broad range of polymer brush architectures

Controlled / "living" radical polymerizations are the predominant technique:

- Compatible with aqueous reaction media
- Broad monomer and functional group scope and tolerance

Surface-Initiated «Living» Polymerizations

Modern living free radical polymerization techniques are based on the use of special polymerization mediators, which temporarily and reversibly transform propagating radicals into dormant species.
This reversible transformation is either accomplished by reversible deactivation or by reversible chain transfer.

Reversible deactivation

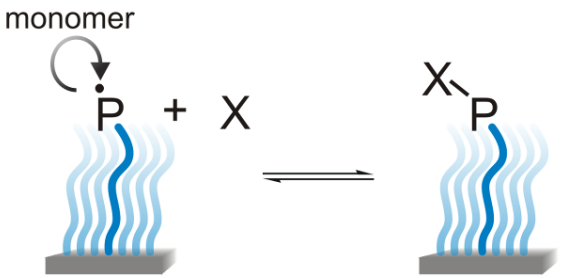

e.g. for SI-NMP or SI-ATRP

Reversible chain transfer

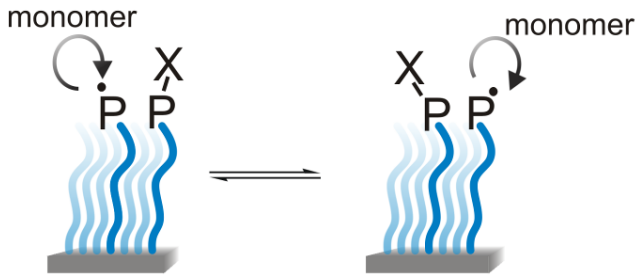

e.g. for SI-RAFT

A fast transformation between dormant and propagating radical species ensures the homogeneous growth of the overall ensemble of polymer chains.

As a result living polymerizations are characterized by:

- a linear evolution of molecular weight with time (for low conversions).
- polydispersity values of typically 1.1.

Surface-Initiated ATRP

Atom transfer radical polymerization (ATRP)

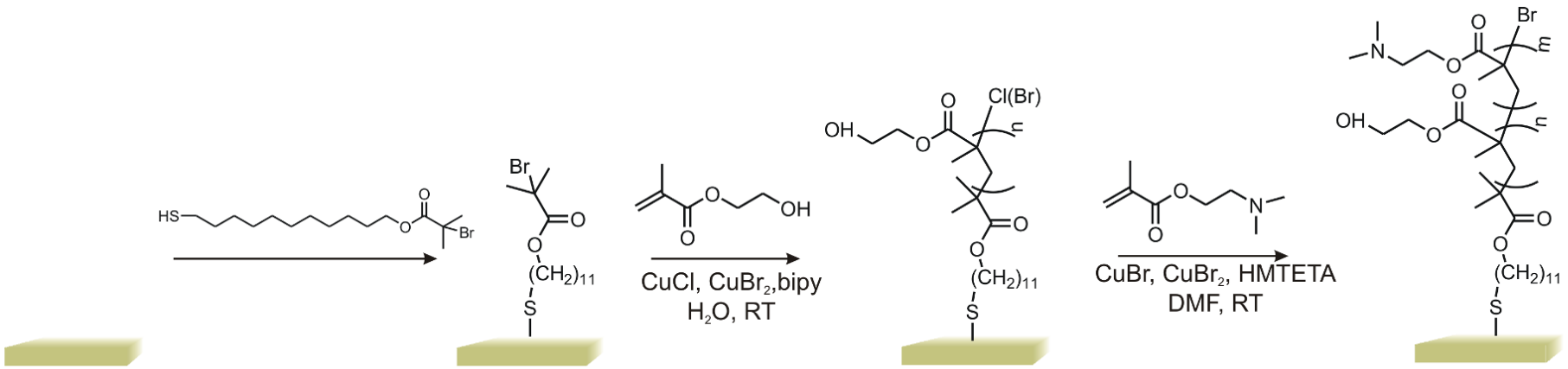

Huang, W.; Kim, J.-B.; Bruening, M. L.; Baker, G. L. *Macromolecules* **2002**, *35*, 1175

SI-ATRP Mechanism

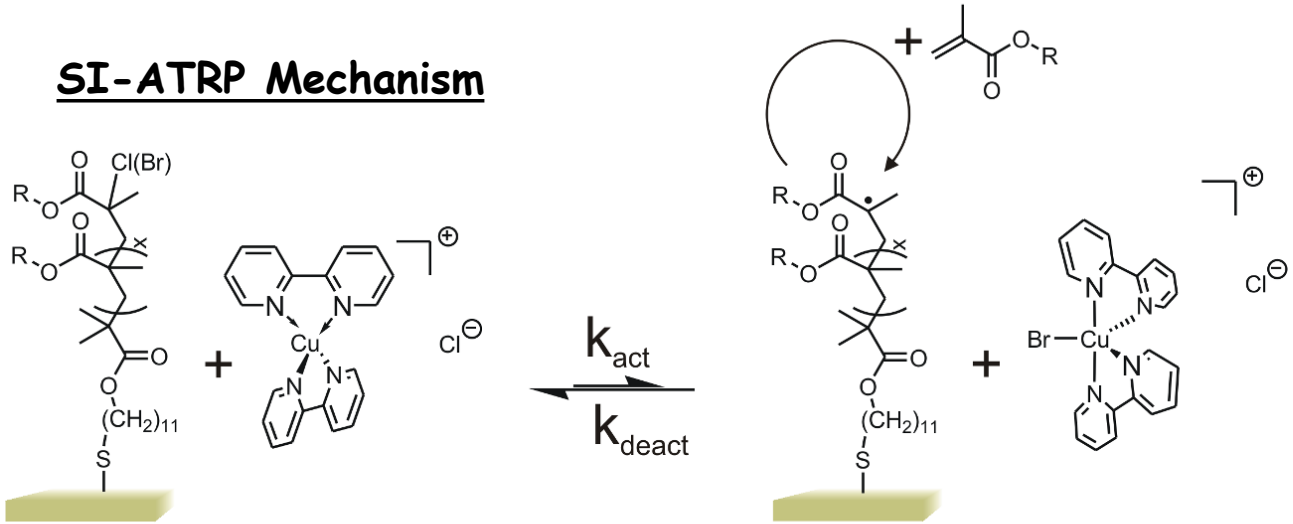

ATRP Ligands

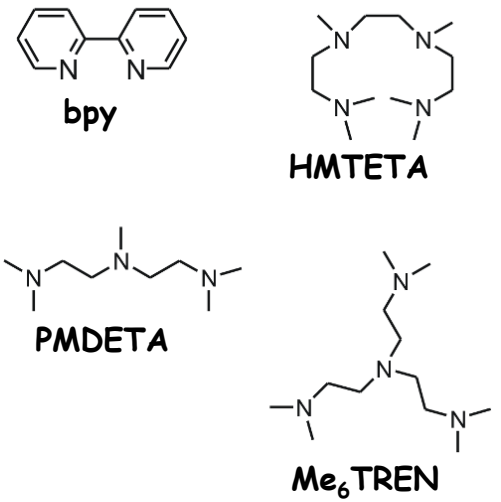

Surface-RAFT Polymerizations

Reversible addition-fragmentation chain transfer polymerization (RAFT)

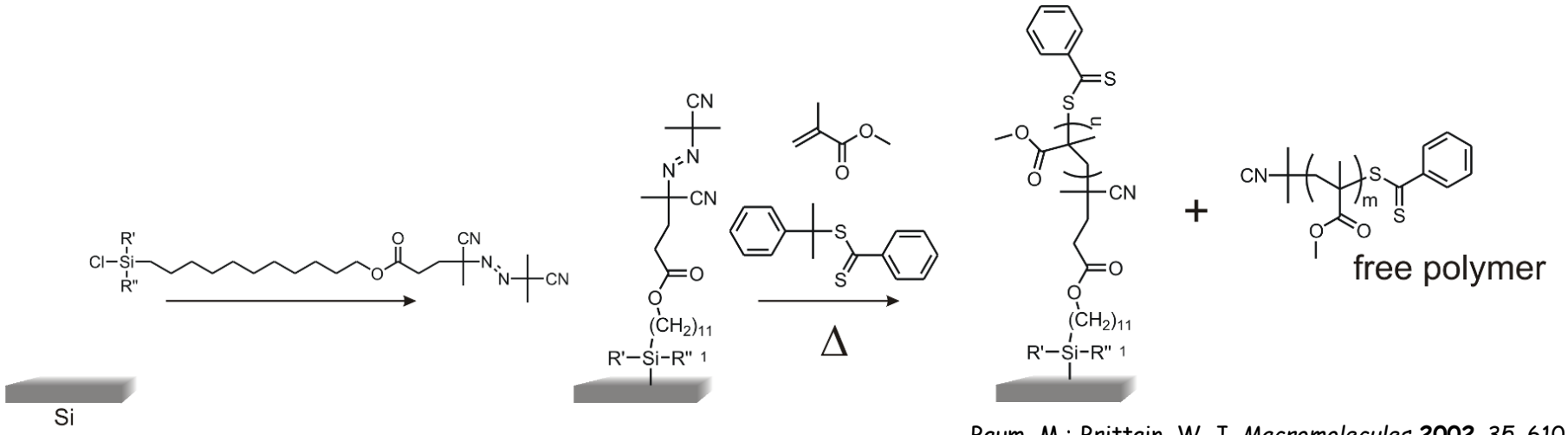

Baum, M.; Brittain, W. J. *Macromolecules* **2002**, *35*, 610

SI-RAFT Mechanism

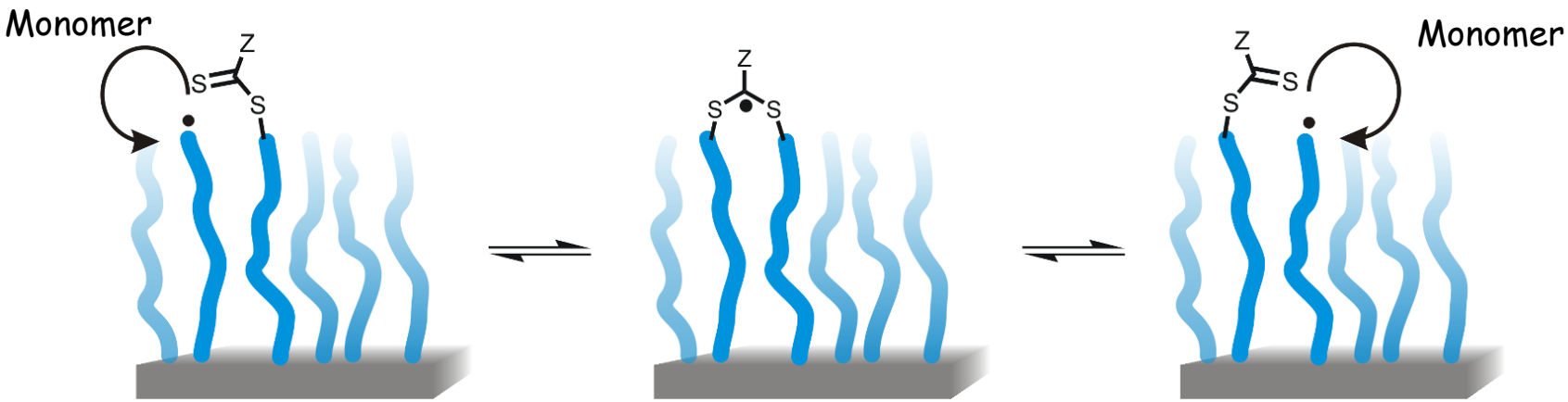

Surface-Initiated NMP

Nitroxide-mediated polymerization (NMP)

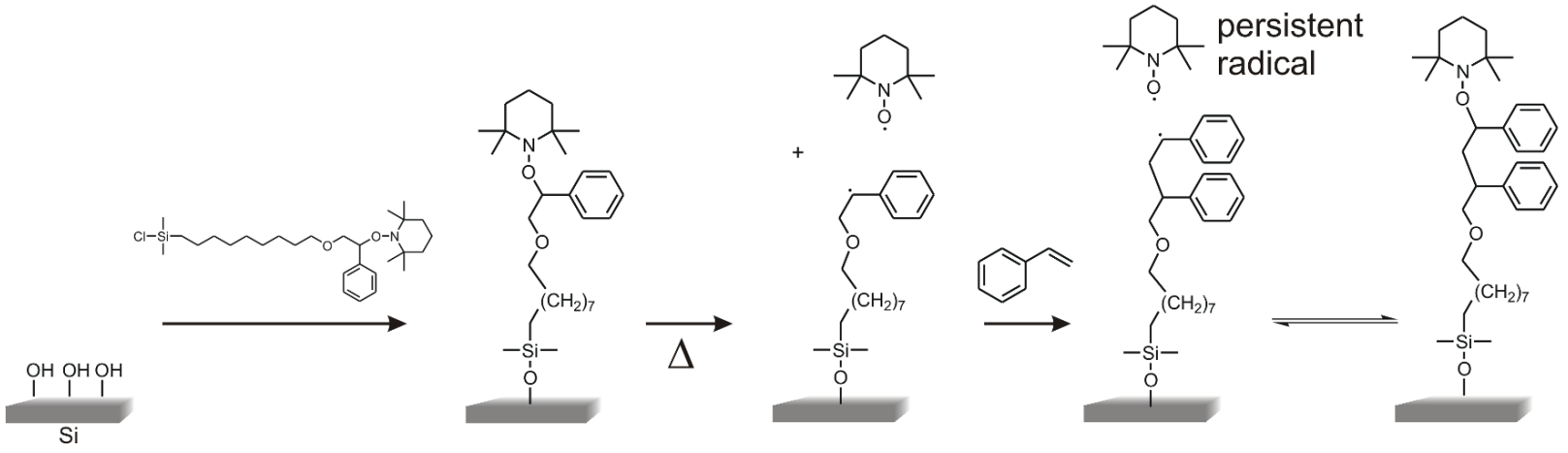

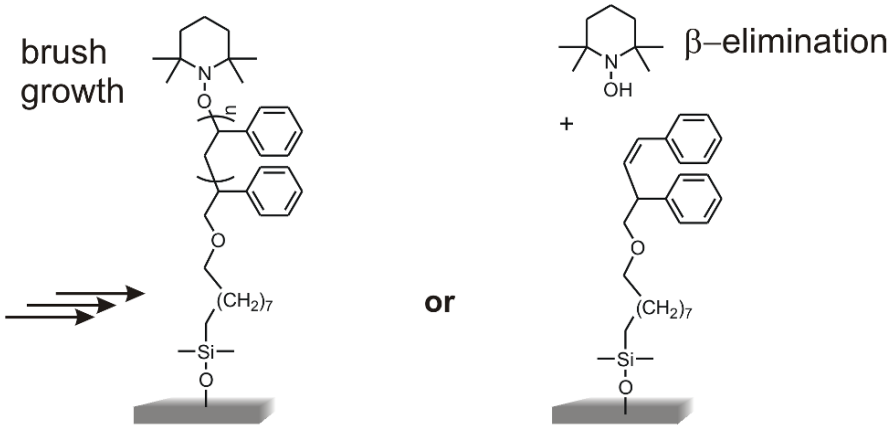

Initiator

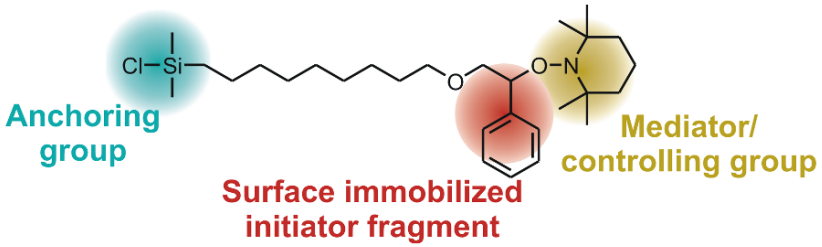

Husseman, M.; Malmström, E. E.; McNamara, M.; Mate, M.; Mecerreyes, D.; Benoit, D. G.; Hedrick, J. L.; Mansky, J. L.; Huang, E.; Russell, T. P.; Hawker, C. J. *Macromolecules* **1999**, *32*, 1424

Control of Polymer Brush Film Thickness

Control of dry film polymer brush thickness via surface-initiated atom transfer radical polymerization

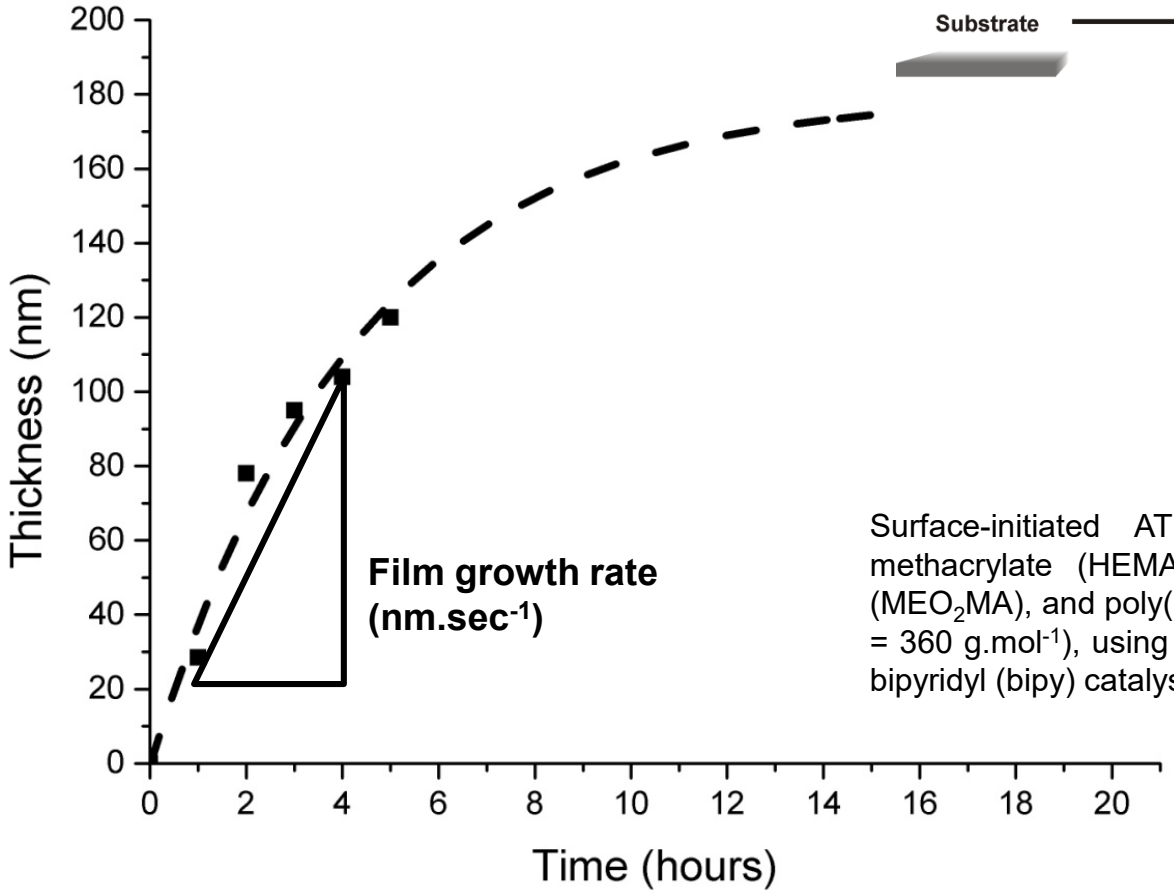

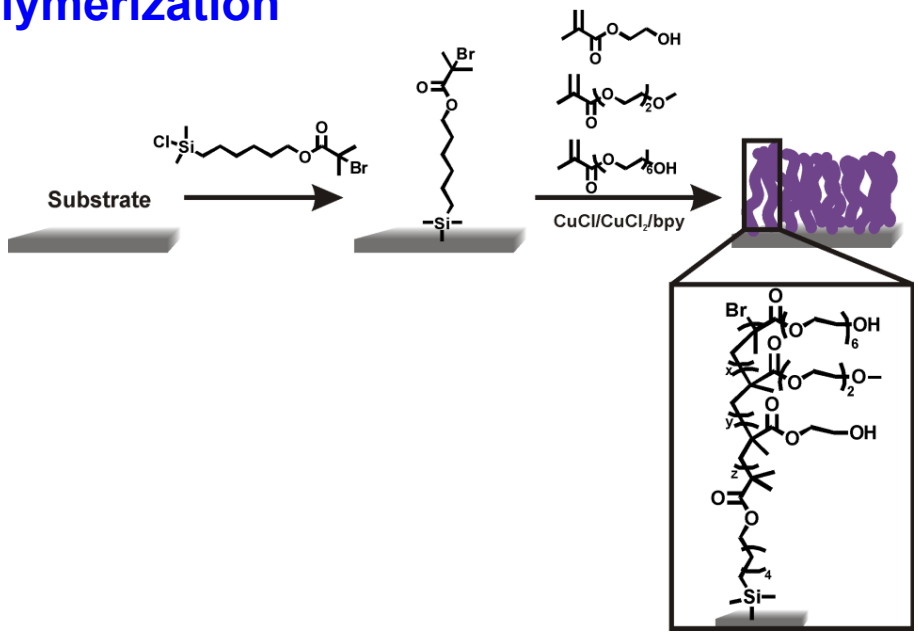

Surface-initiated ATRP copolymerization of 2-hydroxyethyl methacrylate (HEMA), 2-(2-methoxyethoxy)ethyl methacrylate (MEO_2MA), and poly(ethylene glycol) methacrylate ($PEGMA_6$, M_n = 360 $g.mol^{-1}$), using a copper(I)chloride, copper(II)chloride, 2,2-bipyridyl (bipy) catalyst system

S. Desseaux, H.-A. Klok, *Biomacromolecules* **2014**, *15*, 3859 – 3865

Grafting Density, Chain Conformation & Dispersity

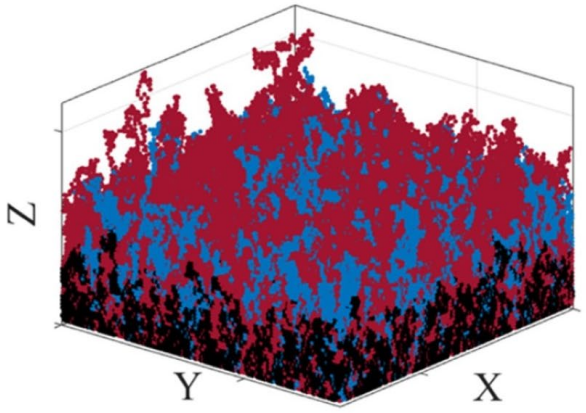

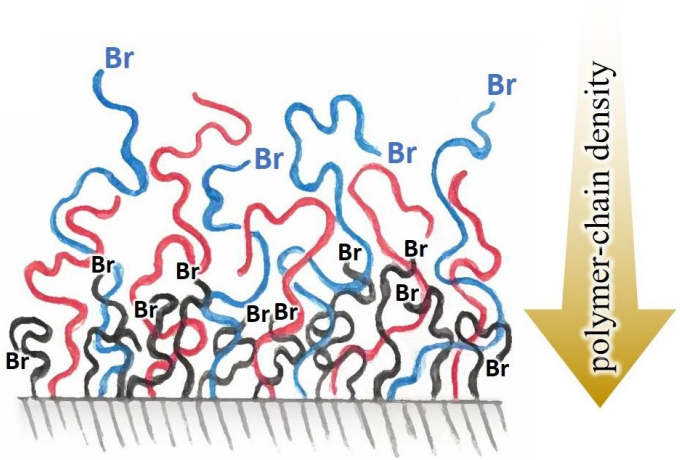

Top: F. J. Arraez, P. H. M. Van Steenberge, J. Sobieski, K. Matyjaszewski, D. R. D'hooge, *Macromolecules* **2021**, *54*, 8270-8288.

Bottom: Image credit: Prof. E. Benetti (Padua)

Grafting density:

- Number of chains anchored to a surface per unit surface area.

Conformation:

- The conformation of a single, surface-anchored polymer chain can be different in proximity of the substrate as compared to the polymer brush - air or polymer brush - solvent interface.
- This is related to the loss of polymerization active chain ends as the brush grows.
- As a consquence, a polymer brush also has a non-uniform density (higher at the interface, and lower at the top).

Dispersity:

- Is related to the «livingness» of the polymerization, and thus influences chain conformation and the polymer brush density profile.

Insights from Computer Simulations

polymers

MDPI

Article

The Competition of Termination and Shielding to Evaluate the Success of Surface-Initiated Reversible Deactivation Radical Polymerization

Francisco J. Arraez [1], Paul H. M. Van Steenberge [1] and Dagmar R. D'hooge [1,2,*]

[1] Laboratory for Chemical Technology, Department of Materials, Textiles and Chemical Engineering, Ghent University, Technologiepark 125, Zwijnaarde, 9052 Ghent, Belgium; franciscojose.arraezhernandez@ugent.be (F.J.A.); paul.vansteenberge@ugent.be (P.H.M.V.S.)

[2] Centre for Textile Science and Engineering, Department of Materials, Textiles and Chemical Engineering, Ghent University, Technologiepark 70A, Zwijnaarde, 9052 Ghent, Belgium

* Correspondence: dagmar.dhooge@ugent.be

Received: 4 June 2020; Accepted: 20 June 2020; Published: 23 June 2020

check for updates

Abstract: One of the challenges for brush synthesis for advanced bioinspired applications using surface-initiated reversible deactivation radical polymerization (SI-RDRP) is the understanding of the relevance of confinement on the reaction probabilities and specifically the role of termination reactions. The present work puts forward a new matrix-based kinetic Monte Carlo platform with an implicit reaction scheme capable of evaluating the growth pattern of individual free and tethered chains in three-dimensional format during SI-RDRP. For illustration purposes, emphasis is on normal SI-atom transfer radical polymerization, introducing concepts such as the apparent livingness and the molecular height distribution (MHD). The former is determined based on the combination of the disturbing impact of termination (related to conventional livingness) and shielding of deactivated species (additional correction due to hindrance), and the latter allows structure-property relationships to be identified, starting at the molecular level in view of future brush characterization. It is shown that under well-defined SI-RDRP conditions the contribution of (shorter) hindered dormant chains is relevant and more pronounced for higher average initiator coverages, despite the fraction of dead chains being less. A dominance of surface-solution termination is also put forward, considering two extreme diffusion modes, i.e., translational and segmental. With the translational mode termination is largely suppressed and the living limit is mimicked, whereas with the segmental mode termination occurs more and the termination front moves upward alongside the polymer layer growth. In any case, bimodalities are established for the tethered chains both on the level of the chain length distribution and the MHD.

Confinement Effects during SI(-ATR)P

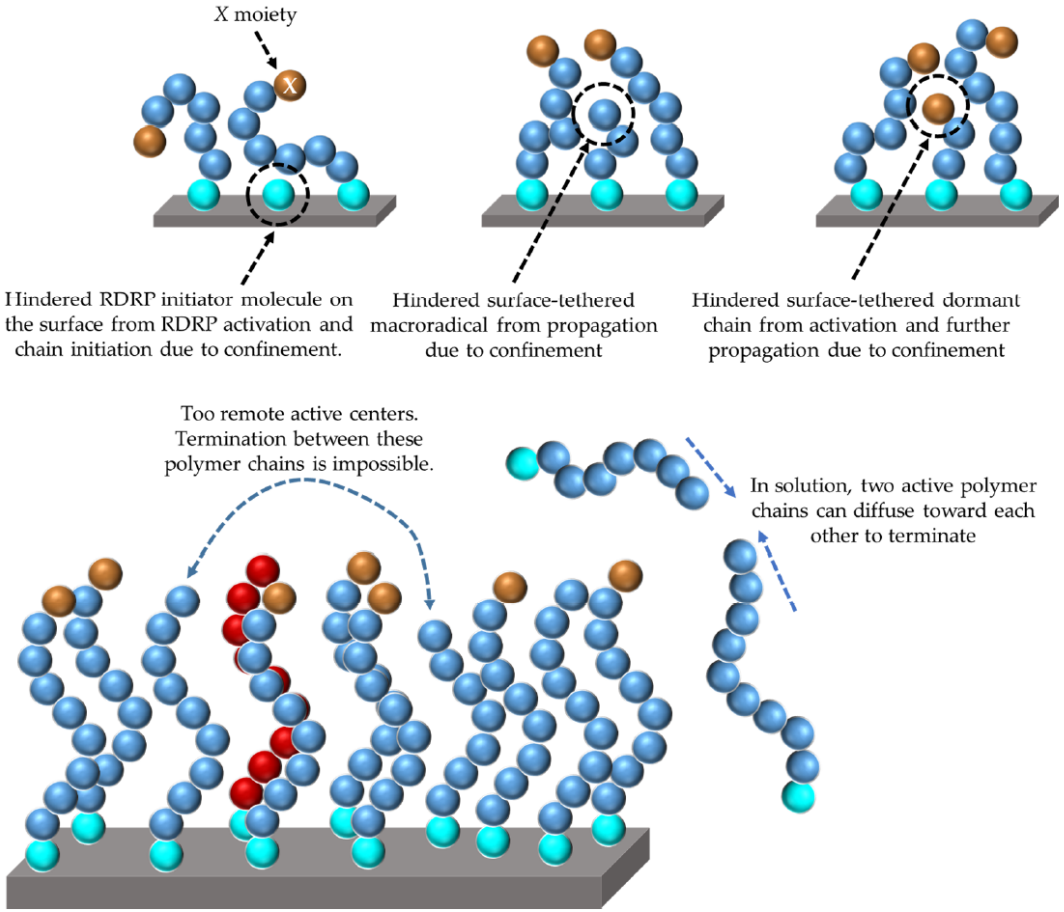

Figure 2. Visualization of confinement in surface initiation—reversible deactivation radical polymerization (SI-RDRP), leading to different reaction probabilities for reactions on the surface and in the solution. For illustration purposes, emphasis is on chain initiation, propagation, activation/deactivation at the top and termination at the bottom. Here, RDRP initiator molecules are represented as cyan spheres, monomer units either in dormant or active polymer chains are represented as blue spheres, and monomer units in dead polymer chains are represented as red spheres. In addition, the "X" chain-ends of dormant polymer chains are depicted as brown spheres to differentiate themselves from the active species.

Macromolecules

pubs.acs.org/Macromolecules Article

Conformational Distributions near and on the Substrate during Surface-Initiated Living Polymerization: A Lattice-Based Kinetic Monte Carlo Approach

Francisco J. Arraez, Paul H. M. Van Steenberge, and Dagmar R. D'hooge*

Cite This: *Macromolecules* 2020, 53, 4630–4648

ABSTRACT: One of the challenges in the field of surface-initiated polymerization (SIP) is gaining access to conformational distributions allowing one to quantify the degree of brush/mushroom character during synthesis. Here, we put forward a novel kinetic Monte Carlo (kMC) tool to be successful in this respect, focusing on chain-to-chain deviations on and near the surface accounting for varying reaction probabilities and combining conventional kMC modeling with a modified version of the bond fluctuation model. The potential of the tool is illustrated for living SIP addressing the effect of shielding on the efficiency of surface initiation and propagation. It is shown that at higher reaction times shielding for propagation leads to the increased formation of hindered shorter chains, causing the formation of a bimodal number chain-length distribution (CLD) for tethered chains compared to the always unimodal number CLD for free larger chains near the surface. Moreover, it can be evaluated at any synthesis time if an individual chain possesses a mushroom, brushlike, or brush conformation. It is demonstrated that an optimal (average) initiator surface coverage exists, leading to a sufficiently high chain grafting density and a maximization of the brush character provided that an initiator with the correct (surface) initiation reactivity is selected. The developed tool is important for the multiangle design of future SIP processes focusing on optimization in reaction time, control over CLD, and conformational features in view of the desired application.

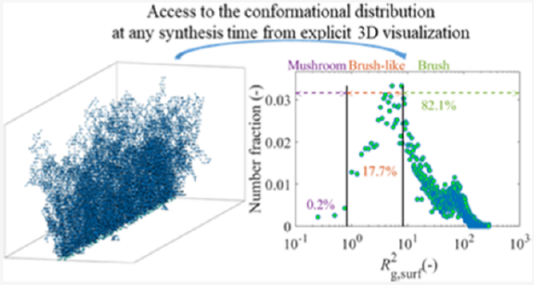

Synthesis of Polymer Brushes

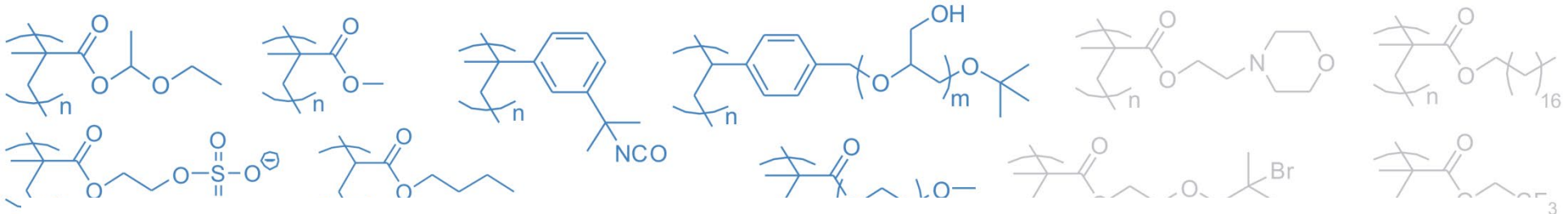

Chem. Rev. **2009,** *109,* 5437–5527

Polymer Brushes via Surface-Initiated Controlled Radical Polymerization: Synthesis, Characterization, Properties, and Applications

Raphaël Barbey, Laurent Lavanant, Dusko Paripovic, Nicolas Schüwer, Caroline Sugnaux, Stefano Tugulu, and Harm-Anton Klok*

École Polytechnique Fédérale de Lausanne (EPFL), Institut des Matériaux, Laboratoire des Polymères, Bâtiment MXD, Station 12, CH-1015 Lausanne, Switzerland

Received February 5, 2009

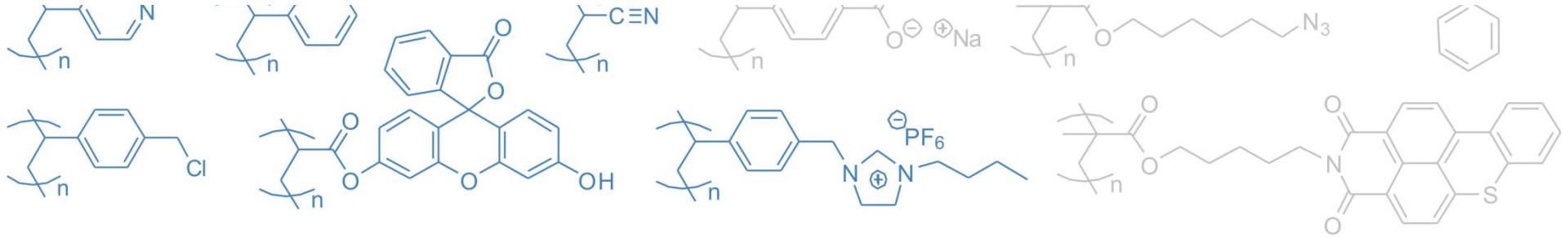

Monomers Polymerized via SIP

			SI-FRP	SI-NMP	SI-ATRP	SI-RAFT	SI-PIMP	SI-AP	SI-CP	SI-ROP	SI-ROMP
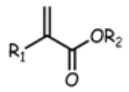	(Meth)acrylates	Neutral	PHEMA, PHEA, PBMA, PDMAEMA, PGMA	PMMA, PBA, PtBA, PDEAEMA	PMMA, PHEMA, PDMAEMA, PtBA, PMA, PEGMA, PEGDMA	PMMA, PBA, PHEMA	PMMA	PMMA			
		Charged	PAA, PMAA		PMAA, PMETAC	PDMAPS					
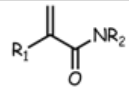	(Meth)acrylamides		PDMA, PAAm	PDMA	PDMA, PNIPAM	PDMA					
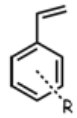	Styrenic monomers	Neutral	PSt	PSt, POEOOMSt	PSt	PSt	PSt	PSt	PSt		
		Charged	PNaSS			PSS					
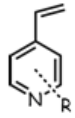	Pyridinic monomers		P4VP	P3VP	P4VP			P2VP			
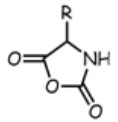	Amino-NCAs									PBLG, PMLG	
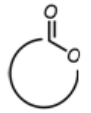	Lactones									PCL, PLA, PDXO	
	Others		PAN					PI, PBD	PIB	PPEI, PEDHO	PBNE, PBNE-d

PHEMA: poly(2-hydroxyethyl methacrylate); **PHEA**: poly(2-hydroxyethyl acrylate); **PBMA**: poly(butyl methacrylate); **PDMAEMA**: poly(2-(dimethylamino)ethyl methacrylate); **PGMA**: poly(glycidyl methacrylate); **PAA**: poly(acrylic acid); **PMAA**: poly(methacrylic acid); **PDMA**: poly(*N*-*N*'-dimethylacrylamide); **PAAm**: poly(acrylamide); **PSt**: polystyrene; PNaSS: poly(styrene sulphonate); **P2VP**: poly(2-vinylpyridine); **P3VP**: poly(3-vinylpyridine); **P4VP**: poly(4-vinylpyridine); **PAN**: poly(acrylonitrile); **PMMA**: poly(methyl methacrylate); **PBA**: poly(butyl acrylate); **PtBA**: poly(*t*-butyl acrylate); **PDEAEMA**: poly(2-diethylamino)ethyl methacrylate); **POEOOMSt**: poly(4-(oligoethyleneoxy)oxymethylstyrene); **PMA**: poly(methyl acrylate); **PEGMA**: poly(oligo(ethyleneglycol) methacrylate): **PEGDMA**: poly(oligo(ethyleneglycol) dimethacrylate; **PMETAC**: poly(2-(methacryloyloxy)ethyltrimethylammonim chloride); **PNIPAM**: poly(*N*-isopropyl acrylamide); **PDMAPS**: poly(N-N'-dimethyl(methylmethacryloyl ethyl)ammonium propane sulfonate); **PSS**: poly(4-styrene sulfonate); **PI**: polyisoprene; **PBD**: poly(butadiene); PIB: poly(isobutylene); **PEDHO**: poly(2-ethyl-4,5-dihydrooxazole); **PPEI**: Poly(N-propionylethyleneimine); **PBLG**: poly(γ-benzyl glutamate); **PMLG**: poly(γ-methyl L-glutamate); **PCL**: poly(caprolactone); **PLA**: poly(L-lactic acid); **PDXO**: poly(1,5-dioxepan-2-one); **PBNE**: polynorbornene; **PNBE-d**: polynorbornene-derived brushes.

Polymer Architectures obtained via SIP

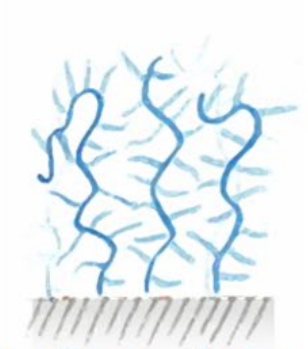

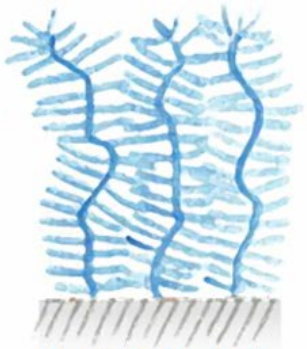

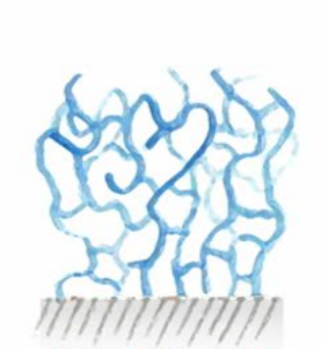

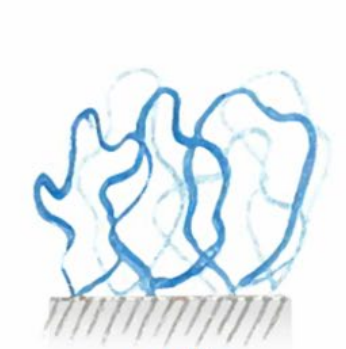

Image credit: Prof. E. Benetti (Padua)

Current Scope and Limitations of SIP

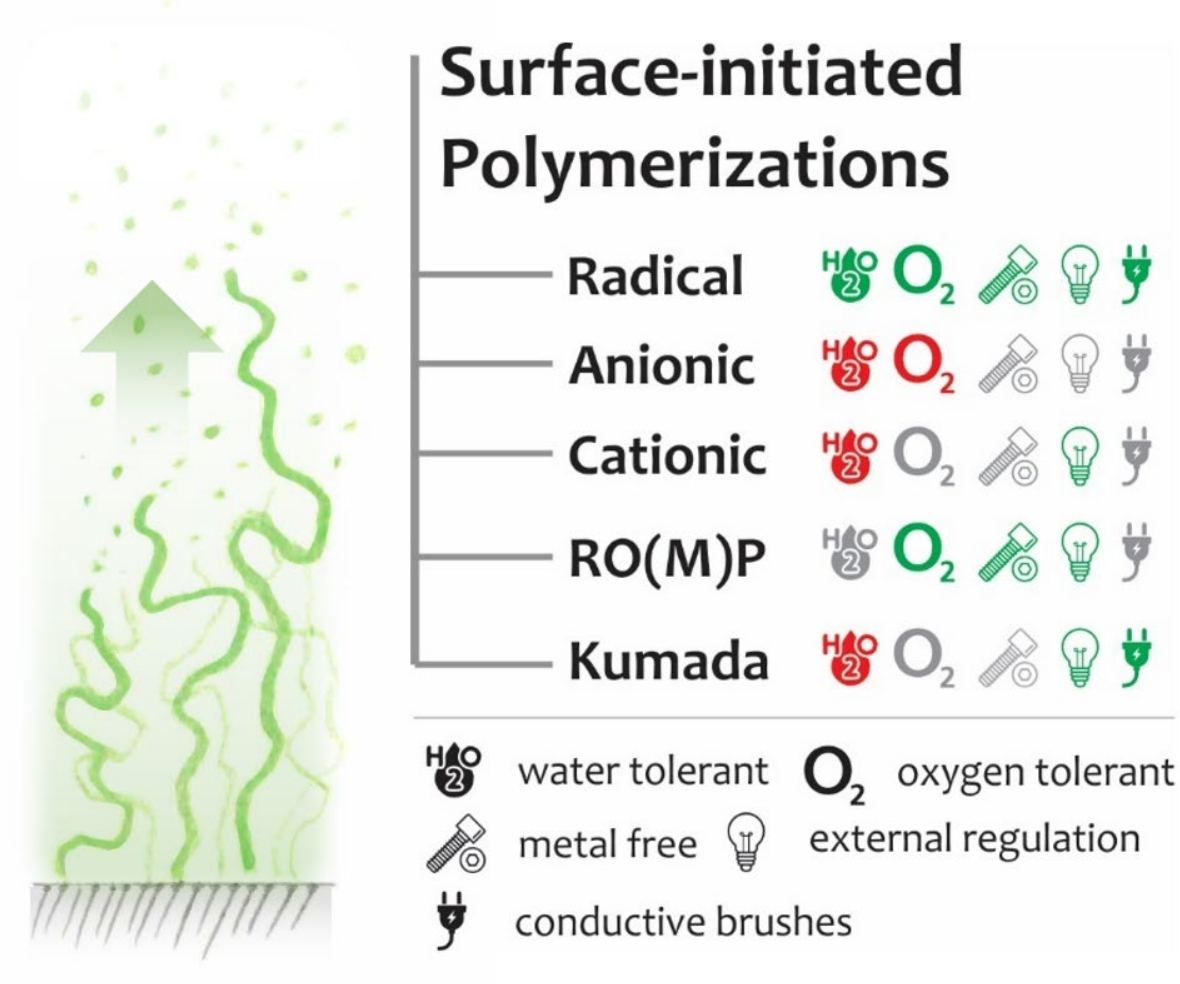

Green color indicates tolerance (*e.g.*, towards H_2O or O_2), **red** specifies inherent chemical incompatibility with previously attempted approaches, and **gray** implies potential possibilities, yet no current literature.

Image credit: Prof. E. Benetti (Padua)

Large Scale SI-ATRP under Ambient Conditions

ACS APPLIED POLYMER MATERIALS

pubs.acs.org/acsapm Article

Surface-Initiated Controlled Radical Polymerization: Going beyond Laboratory Scale

Jakob Pagh Nikolajsen, Lukas Vogtmann Thinnesen, Orhan Altuğ Karabiber, Kim Daasbjerg, Steen Uttrup Pedersen, Mikkel Kongsfelt, and Mie Lillethorup*

Cite This: *ACS Appl. Polym. Mater.* 2023, 5, 3534–3541 Read Online

ACCESS | Metrics & More | Article Recommendations | Supporting Information

ABSTRACT: Surface coatings of immobilized polymer brushes are used, e.g., as lubricants, for anti-fouling, and as adhesives. Based on surface-initiated controlled radical polymerization (SI-CRP), a fast, versatile, and enduring scaled SI-CRP ($SI\text{-}CRP_{scaled}$) approach for the formation of polymer brushes is reported. The chemical process is made from an easily prepared chemical solution that is reusable for more than 6 h, even in the presence of oxygen. Because an inert atmosphere is not required, the $SI\text{-}CRP_{scaled}$ process can be carried out under ambient conditions with no significant loss of polymerization activity and viability. The high bath life of the activated solution along with an extraordinarily high brush growth rate of 10 nm per minute makes this method industrially relevant. Based on a straightforward dip coating protocol, this is the first scaled polymer brush technique successfully demonstrated on an industrial scale, enabling uniform polymer brush-functionalized materials for a broader variety of applications.

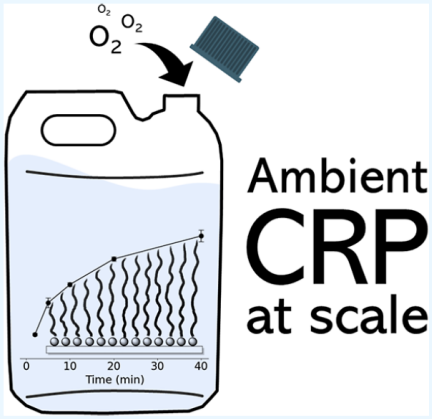

KEYWORDS: *polymer brushes, surface-initiated controlled radical polymerization (SI-CRP), thin films, long-lived, industrial scale*

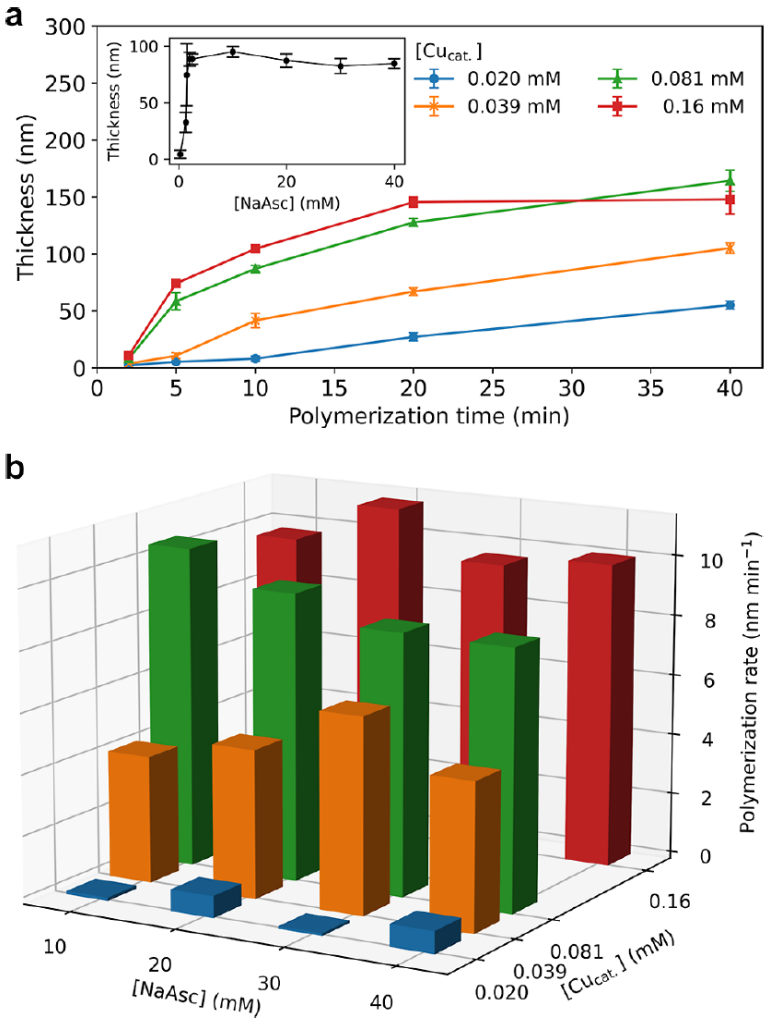

Figure 1. (a) Polymer brush thickness on a stainless-steel substrate as a function of polymerization time for SI-CRP$_{scaled}$ comprising [MMA] = 0.7 M, [NaAsc] = 20 mM, and [Cu$_{cat}$] = 0.020 (●), 0.039 (×), 0.081 (▲), and 0.16 mM (■) in 100 mL water/ethanol (v/v = 1.3:1); inset shows polymer brush thickness vs [NaAsc] using [Cu$_{cat}$] = 0.081 mM; lines drawn to guide the eye. (b) Polymerization rates derived from data presented in (a) and Figure S1, calculated from the initial 10 min of polymerization. All data including standard deviations are available in the Supporting Information (Table S1).

CONCLUSIONS

In summary, we have demonstrated the potential of the SI-CRP technology at scale because of its good tolerance toward oxygen, high control of polymerization, fast polymerization rates, monomer versatility, and simple production setups. On the basis of the general PMMA protocol, we achieved a polymerization rate of ~10 nm min^{-1}, exceeding similar polymerization rates for SI-polymer brushes in the literature. SI-CRP$_{scaled}$ was shown to be compatible with a wide range of monomers, including GMA, HFDMA, ST, PFS, and HEMA. Furthermore, the DOE approach was used to optimize the polymerization with respect to concentrations of reactants, solvent systems, and oxygen reduction, thereby making it applicable for multiple uses over a bath life as long as 6 h. Finally, the potential for industrialization of SI-CRP$_{scaled}$ was demonstrated by treating five batches of 50 A5-size samples with 10 min polymerization time per batch in a 10 L polymerization solution. Altogether, we succeeded in coating 250 samples with ~90 nm thick polymer brushes within 55 min, which is the first demonstrated use of a SI-CRP solution on such a scale.

Macromolecules

Article

Cite This: *Macromolecules* 2018, 51, 10065−10073

pubs.acs.org/Macromolecules

Sol−Gel Preparation of Initiator Layers for Surface-Initiated ATRP: Large-Scale Formation of Polymer Brushes Is Not a Dream

Tomoya Sato, Gary J. Dunderdale, Chihiro Urata, and Atsushi Hozumi*

National Institute of Advanced Industrial Science and Technology (AIST), 2266-98, Anagahora, Shimoshidami, Moriyama, Nagoya 463-8560, Japan

Supporting Information

ABSTRACT: We demonstrated for the first time a facile and reproducible preparation of large-scale (~40 m^2) initiator layers for surface-initiated atom transfer radical polymerization (SI-ATRP) using a simple sol−gel solution of (*p*-chloromethyl)phenyltrimethoxysilane and tetraethoxysilane. Highly smooth and transparent initiator layers could be formed on various inorganic/organic substrates via a spin-, wire-bar-, or roll-to-roll-coating without any marked change in surface morphology or bulk properties at room temperature. Combining the advantages of this sol−gel approach and subsequent "paint on" SI-ATRP using a variety of waterborne monomers, we have succeeded in the formation of polymer brushes on large-scale real-life substrates (i.e., maximum 50 × 50 cm^2) under ambient conditions (room temperature and open to the air) without any complicated apparatus or harsh reaction conditions.

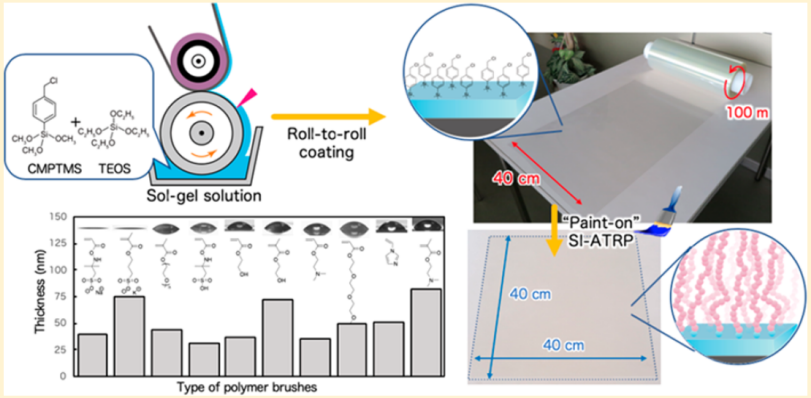

"Paint on" SI-ATRP

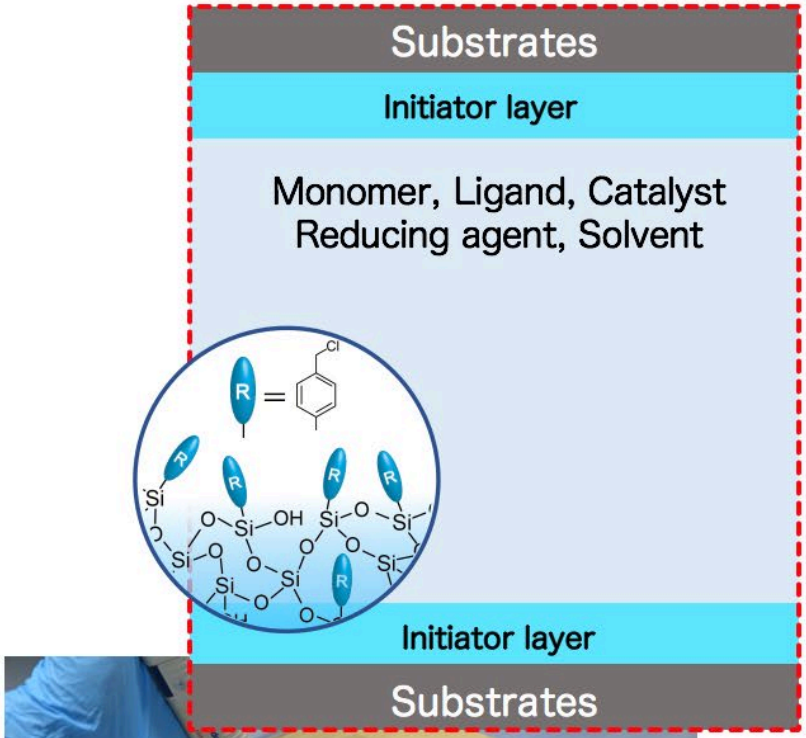

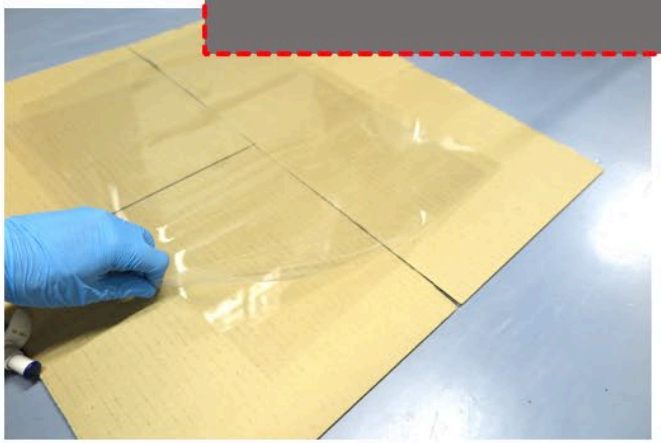

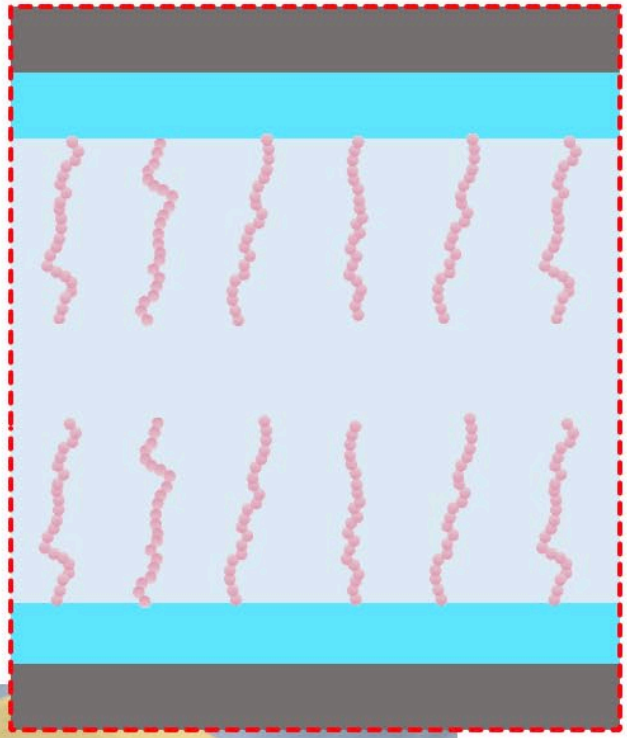

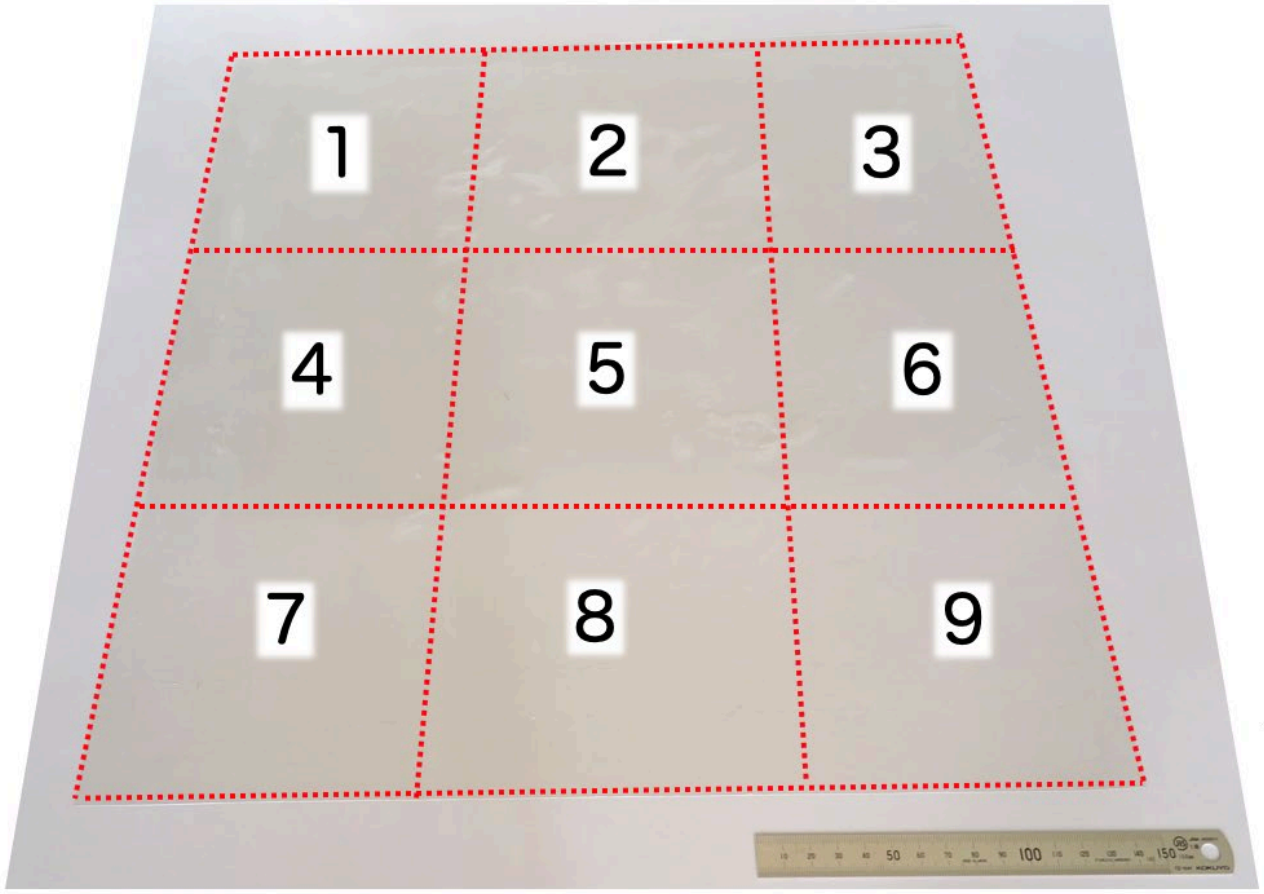

Area No.	Thickness (nm)	Water θ_S (°)
1	87.2	53
2	78.7	53
3	79.0	52
4	79.5	55
5	85.8	52
6	76.4	55
7	76.1	55
8	79.6	55
9	74.5	54
Average	79.7	54

Figure S6. Average dry thicknesses and water θ_S values measured at nine different points on *p*DMAEMA brushes grafted from *i*CMPTMS-covered PET roll film (roll-to-roll coating, 40 × 40 cm^2).

ACS APPLIED MATERIALS & INTERFACES

Letter

www.acsami.org

Large-Scale and Environmentally Friendly Synthesis of pH-Responsive Oil-Repellent Polymer Brush Surfaces under Ambient Conditions

Gary J. Dunderdale, Chihiro Urata, Daniel F. Miranda, and Atsushi Hozumi*

Materials Research Institute for Sustainable Development, National Institute of Advanced Industrial Science and Technology (AIST), 2266-98 Anagahora, Shimoshidami, Moriyama, Nagoya 463-8560, Japan

Supporting Information

ABSTRACT: Contrary to conventional ATRP, aqueous A(R)GET-ATRP at ambient temperature without deoxygenating reaction solutions is an extremely facile method to create polymer brushes. Using these techniques, extremely thick poly[2-(dimethylamino)ethyl methacrylate] polymer brushes can be prepared (~700 nm), or reaction solutions can be low chemical-content, consisting of 99% v/v water. Based on these techniques, we have also developed an easy and inexpensive method, referred to as "paint on"-ATRP, that directly pastes reaction solutions onto various large-scale real-life substrates open to the air. The resulting brush surfaces possess excellent oil-repellent properties, which can be activated or deactivated in response to solution pH.

KEYWORDS: *poly[2-(dimethylamino)ethyl methacrylate], polymer brush, ARGET-ATRP, superoleophobic, pH-responsive, large scale*

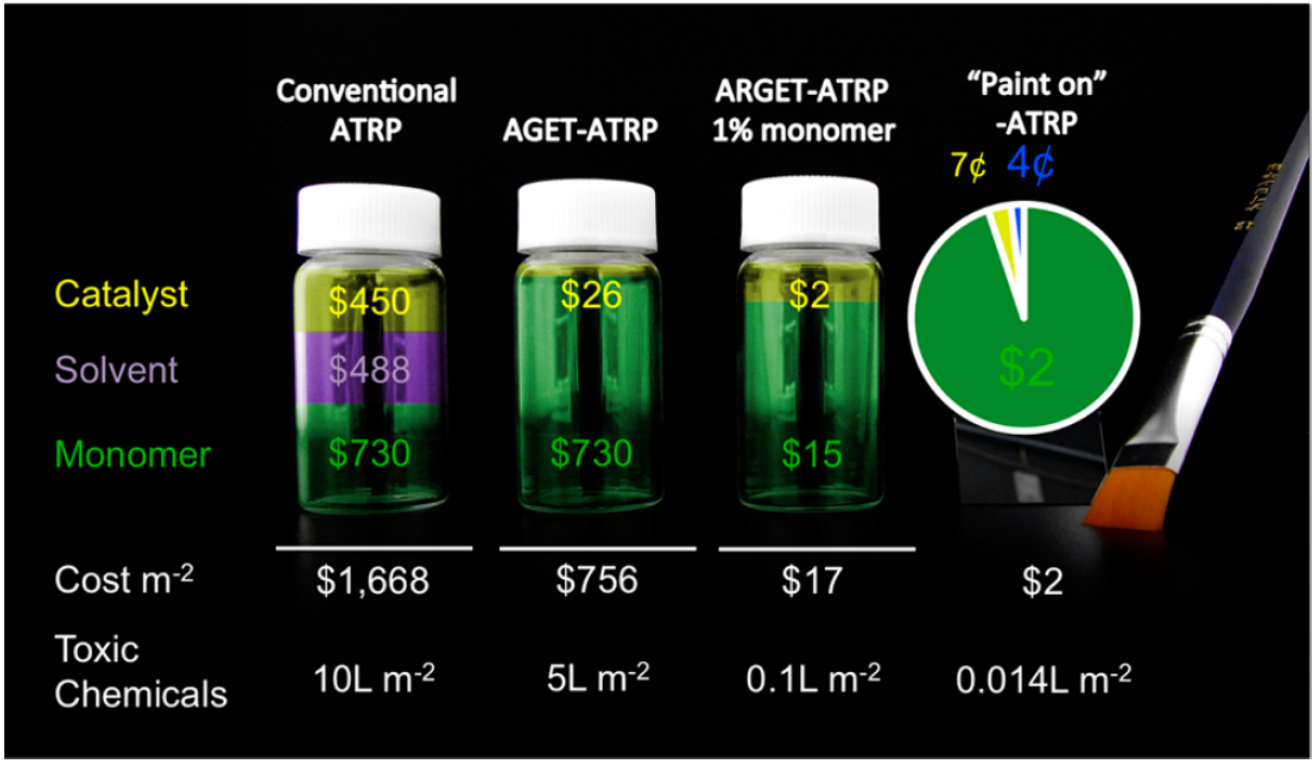

Figure 2. Costs of polymer brushes created using conventional ATRP, AGET-ATRP, ARGET-ATRP and "paint on"-ATRP. Green indicates cost of monomer, purple cost of organic solvent, yellow cost of catalyst, and blue cost of ascorbic acid. The total cost per square meter is shown at the bottom, along with the amount of toxic chemicals used.

What is a polymer brush (and when is a brush a brush….)?

Making polymer brushes

Characterizing polymer brushes

What are polymer brushes good for ?

Chemical Composition

FTIR Spectroscopy

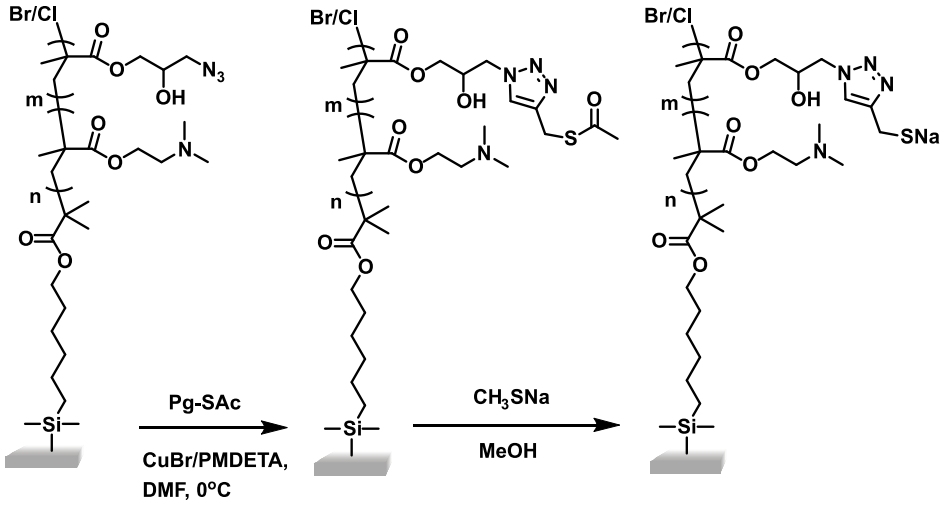

mol % AzHPMA in monomer feed	50 %	10 %	5 %	1 %
N_3 Brush	■	■	■	■
Thioacetate brush	●	●	●	●
Thiol brush	▲	▲	▲	▲

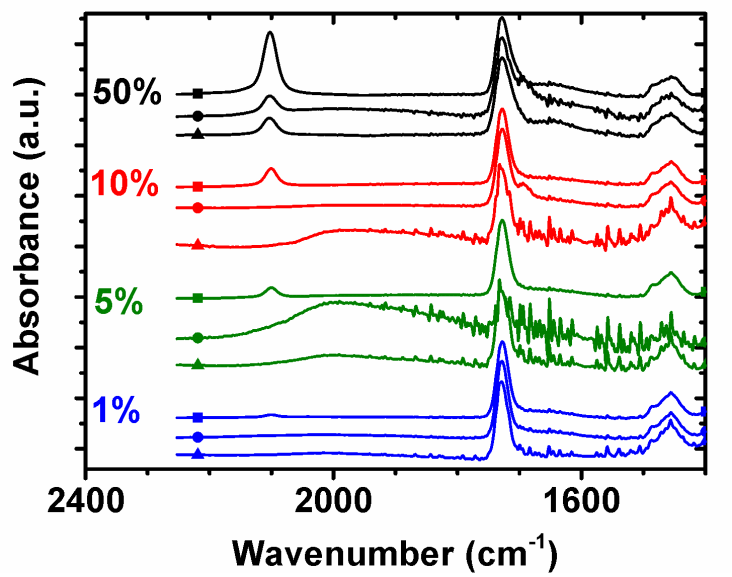

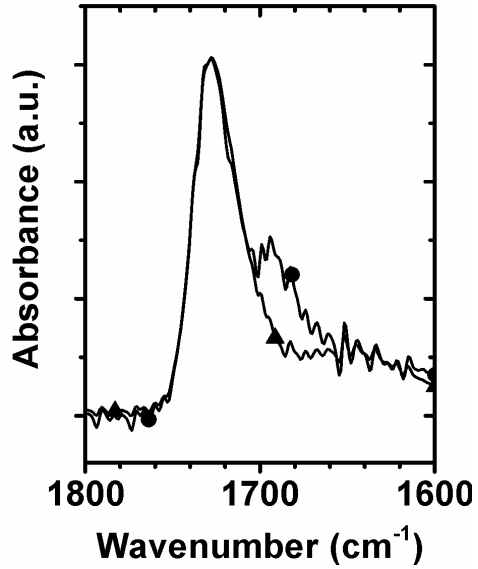

P. Mocny, H.-A. Klok, *Macromolecules* **2020**, *53*, 731

X-Ray Photoelectron Spectroscopy (XPS)

Photoelectric effect

Einstein, Nobel Prize 1921

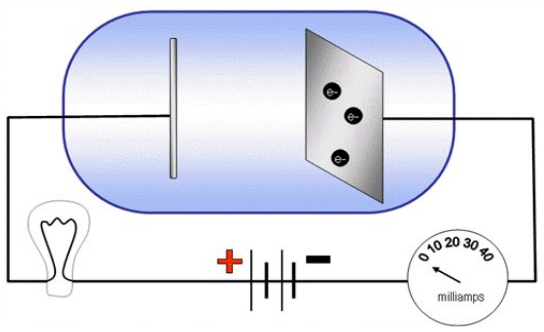

Photoelectric effect

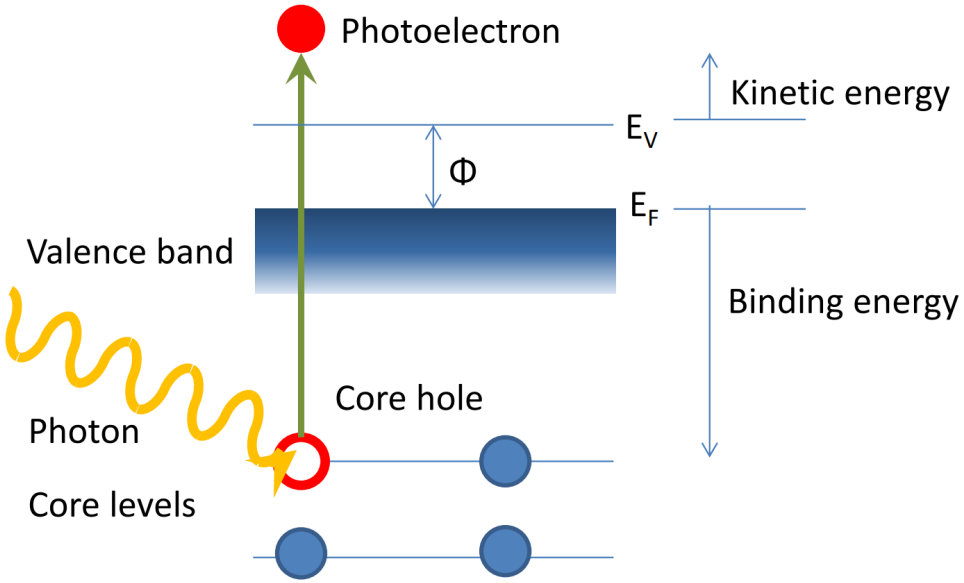

KE=*hv*-BE-φ

***hv*: Incident light energy (known)**

KE: Kinetic energy (measured)

BE: Binding energy (calculated)

φ: Photoelectric workfunction (known)

XPS is also referred to as Electron Spectroscopy for Chemical Analysis (ESCA)

https://steemit.com/science/@shehzad/photoelectric-effect-and-photocells

X-Ray Photoelectron Spectroscopy (XPS)

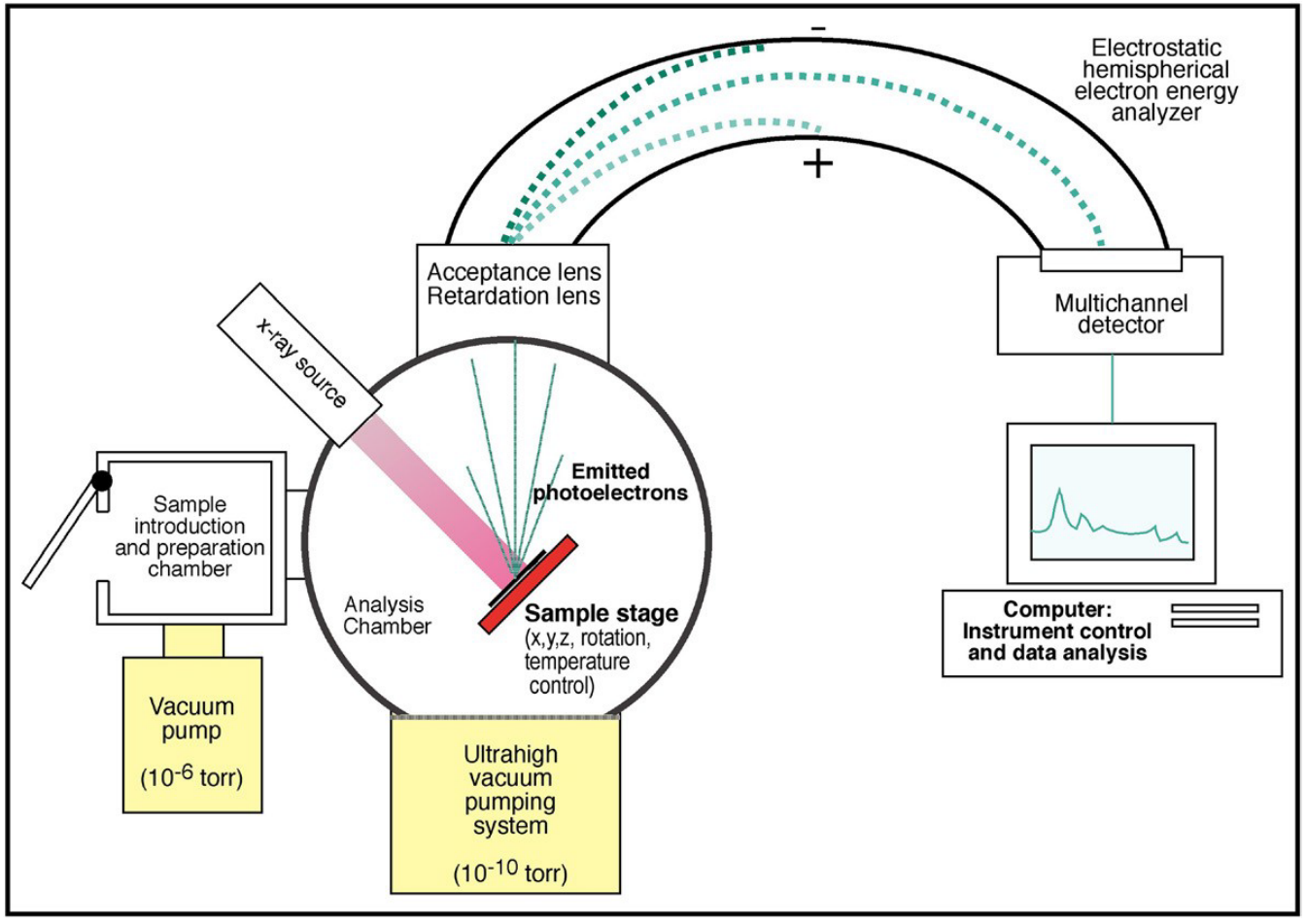

FIGURE I.1.5.6 Schematic diagram of a mono- chromatized ESCA instrument.

Ch. 1, Buddy D. Ratner, A. S. Hoffman, Frederick J. Schoen, J. E. Lemonds, Biomaterials Science, 2nd edition (Wiley)

XPS-Data analysis

Binding energy is determined by
1: Interaction between electron and nucleus (type of element).
2: Chemical bonding state.

Different element

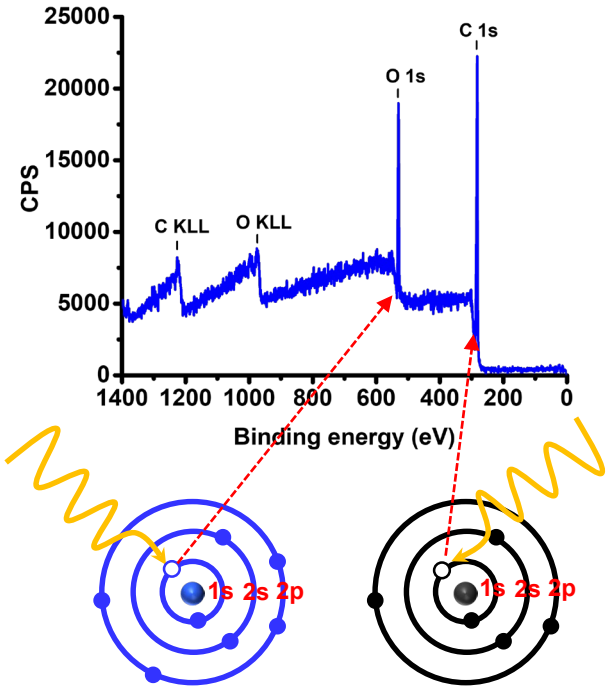

Different chemical state
Intensity ∝ concentration

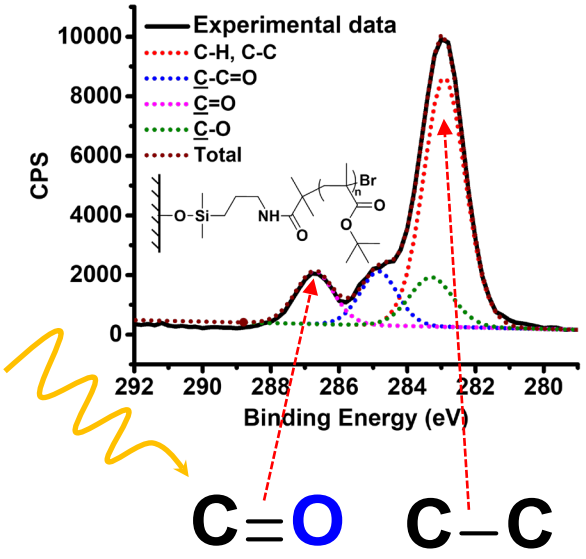

XPS can be used to analyze:
1: Elemental identification and chemical state of element.
2: Relative composition of the constituents in the surface region.

J. Wang, H.-A. Klok, *Angew. Chem. Int. Ed.* **2019**, *58*, 9989
D. Son et al, *Polymers* **2020**, 12, 1053

Brush Functionalization

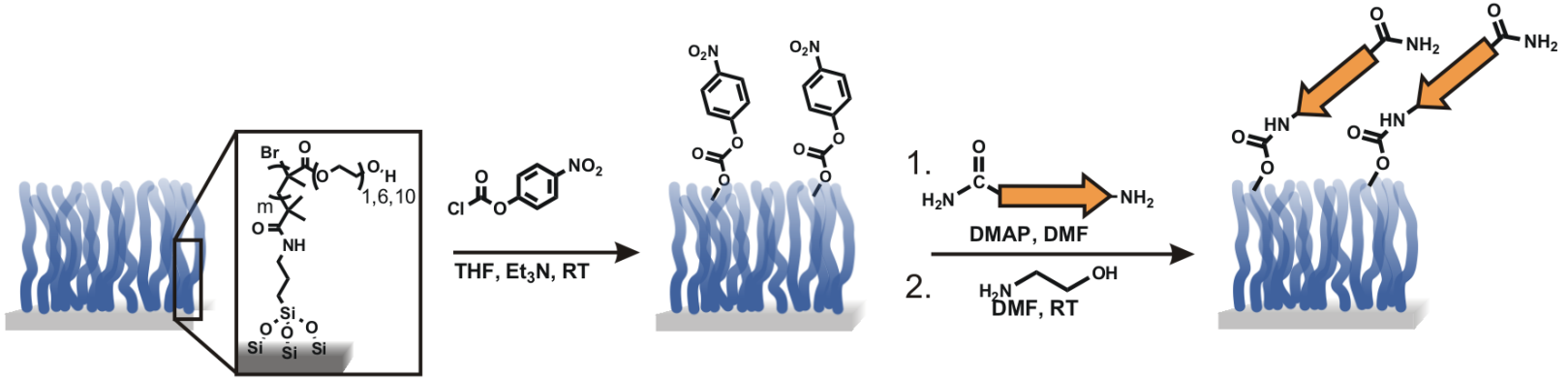

Cell Adhesion:

RGD

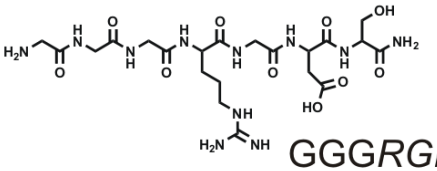

GGG*RGDS*

Negative Control:

R*DG*

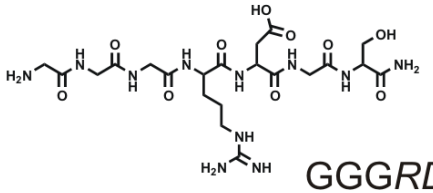

GGG*RDGS*

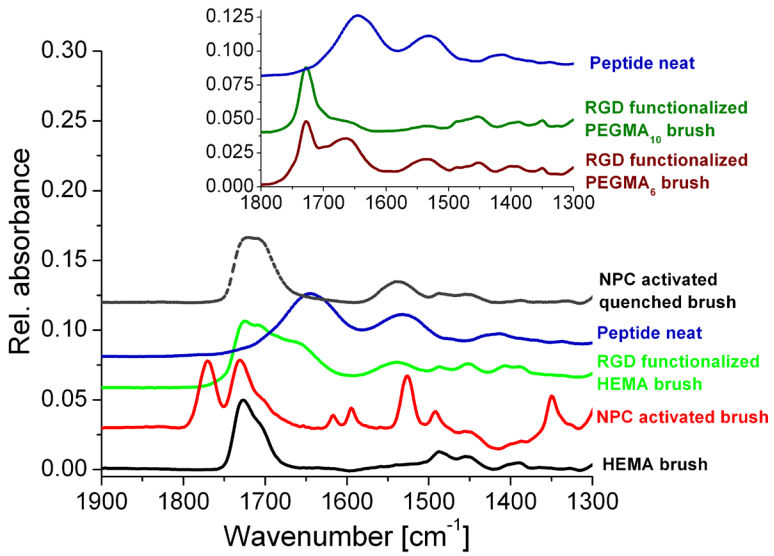

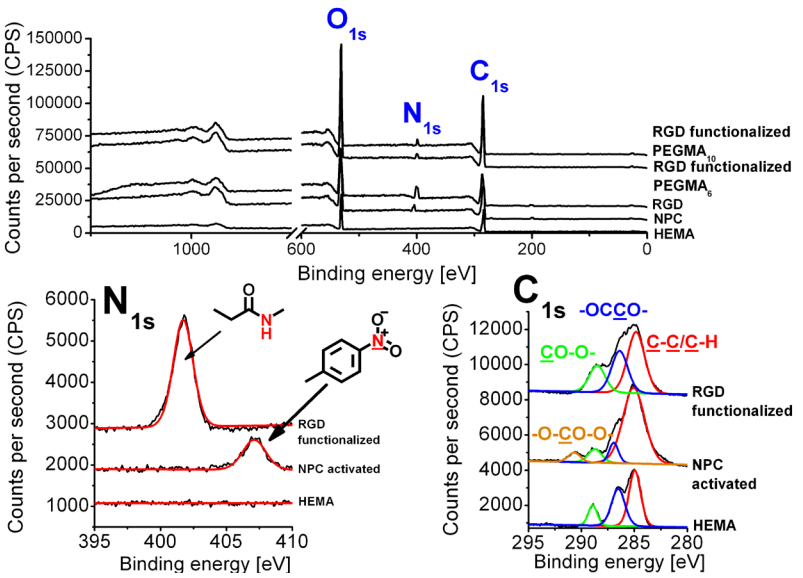

S. Tugulu, P. Silacci, N. Stergiopulos, H.-A. Klok, *Biomaterials* **2007**, *28*, 2536

Characterization of Structural Parameters

Key structural parameters of polymer brushes are the **molar mass** of the surface-anchored polymers, and the **grafting density** (σ).

Grafting density (nm^{-2}):

$$\sigma = \frac{h\,\rho\,NA}{M_n}$$

h: dry film thickness of the brush
ρ : polymer density
$N_{A:}$ Avogadro's constant
M_n: number-average molecular weight of the polymer grafts

When the dry film thickness or mass of polymer brushes are known, any experiment that provides information about σ also affords the M_n of the polymer grafts, and vice versa.

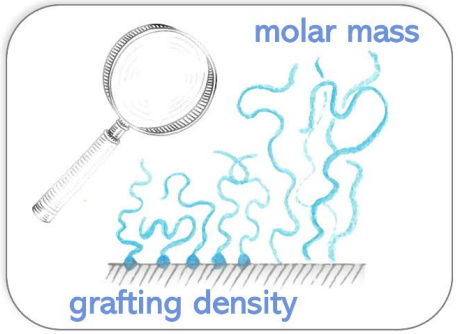

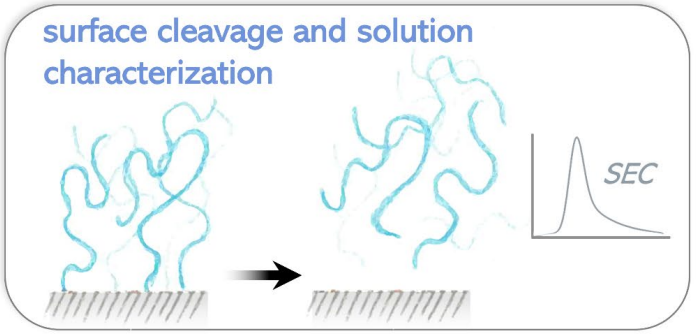

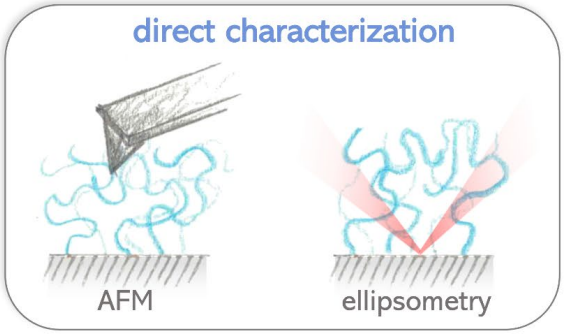

Image credit: Prof. E. Benetti (Padua)

Determining Polymer Brush Dry Film Thickness

Polymer brushes grafted from or onto nanoparticles:

- Thermogravimetric analysis (TGA)

Polymer brushed grafted from or onto planar substrates:

- Atomic force microscopy (on patterned brushes)
- Ellipsometry

TGA of Polymer Brush Grafted Nanoparticles

Scheme 1. Synthesis of Loop PMMA Brushes via SI-ATRP of MMA and Subsequent Chain-End Modification and Loop-Closure Metathesis

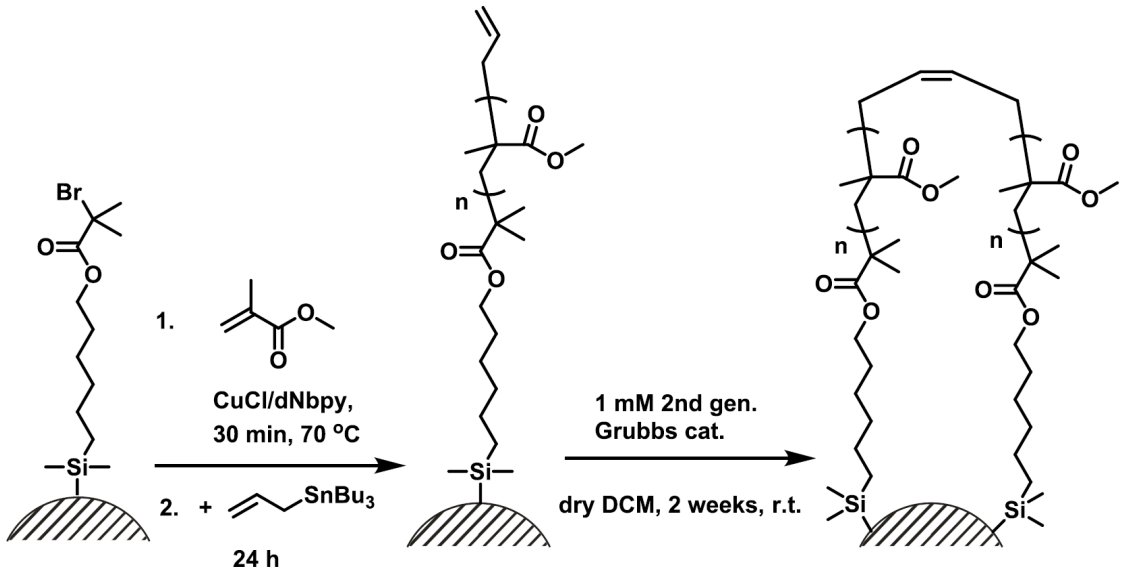

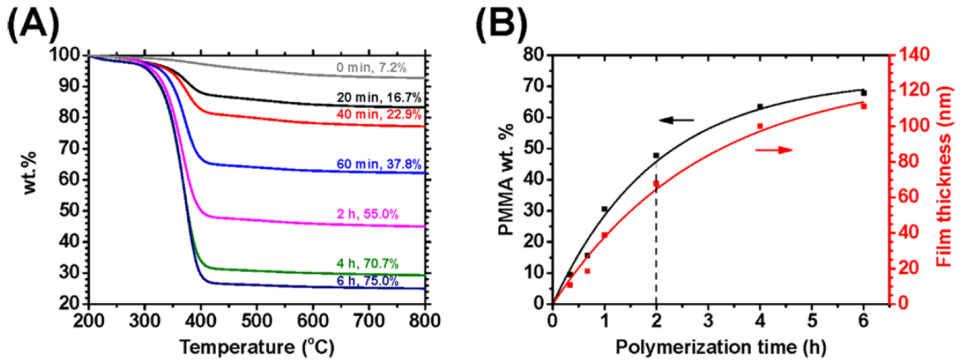

Figure 2. (A) TGA curves of PMMA-grafted silica nanoparticles (ϕ = 332 nm) prepared by SI-ARGET-ATRP at different polymerization times. A heating ramp of 10 °C/min was used. (B) TGA weight loss between 200 and 800 °C and dry PMMA brush film thicknesses as a function of polymerization time.

P. Mocny, M. Ménetrey, H.-A. Klok, *Macromolecules* **2019**, *52*, 8394 – 8403

AFM Analysis of Micropatterned Polymer Brushes

Instead of this “bottom up” approach, sometimes a simple scratch can also work

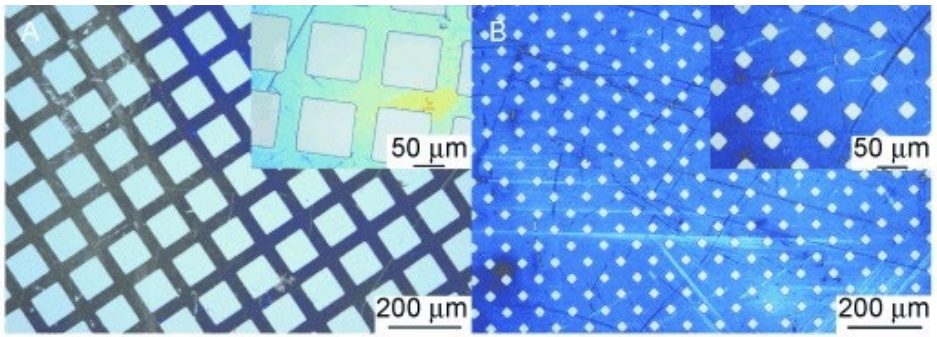

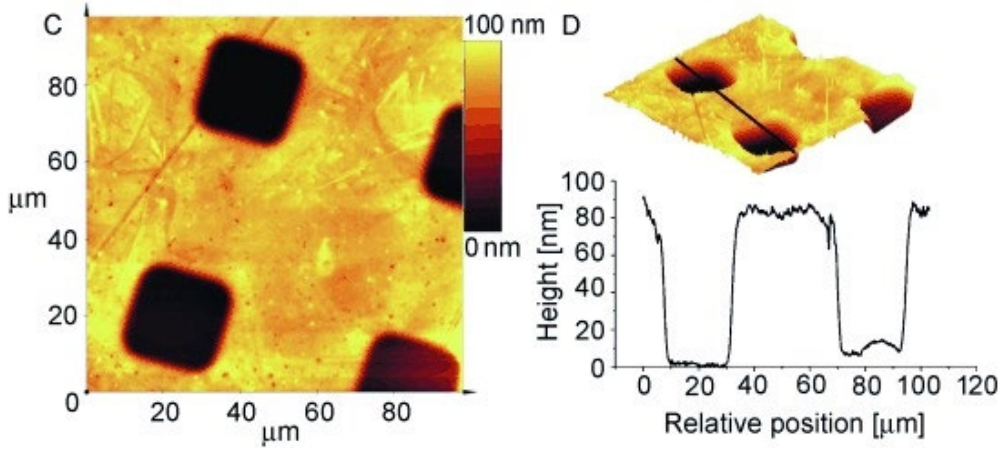

S. Tugulu, M. Harms, M. Fricke, D. Volkmer, H.-A. Klok, *Angew. Chem. Int. Ed.* **2006**, *45*, 7458 – 7461

Ellipsometry – Interaction of Light and Matter

Polarized light interacts with sample upon reflection

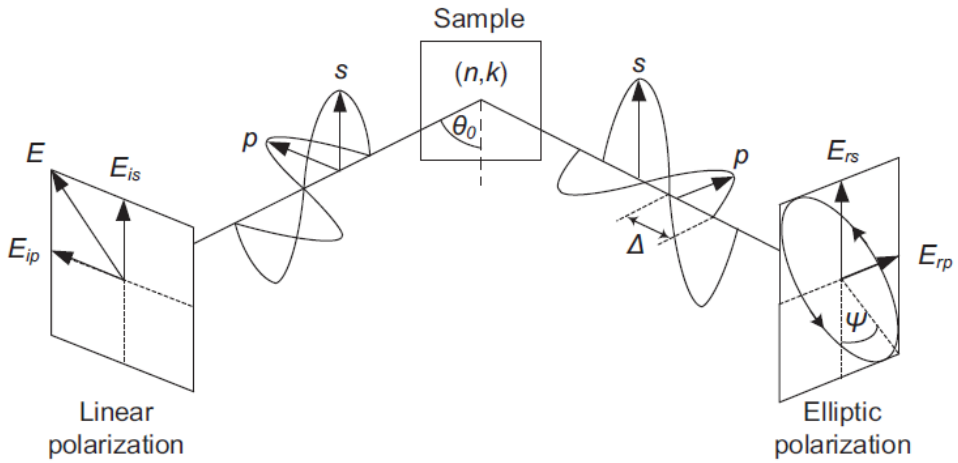

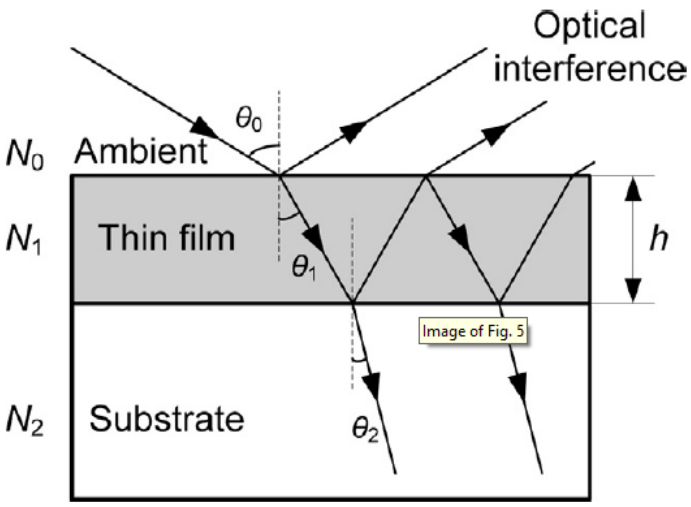

Complex reflectance ratio

$$\rho = \frac{r_s}{r_p} = \tan\Psi * e^{i\Delta}$$

r_s *and* r_p: *amplitudes of s and p component, after reflection normalized to their initial value*

Ψ : *amplitude ratio upon reflection*

Δ : *phase shift*

The change of polarization upon reflection on the surface can be expressed in terms of the two angles Ψ and Δ, which is the typical outcome of an ellipsometric measurement, usually measured as a function of wavelength, angle of incidence or both.

W. Ogieglo et al., *Progress in Polymer Science* **2015**, 42, 42
H. Fujiwara, I. Wiley, Spectroscopic ellipsometry principles and applications, John Wiley & Sons, **2007**
H. G. Tompkins and W. A. McGahan, Spectroscopic ellipsometry and reflectometry : a user's guide, **1999**

Ellipsometry – Data Fitting

Structure of sample has to be known or needs to be assumed

most models are based on the assumption that the sample is composed of a **small number of discrete, well-defined layers that are optically homogeneous and isotropic**

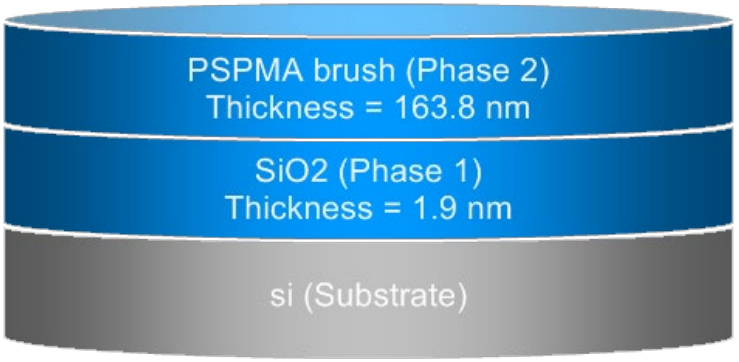

The complex reflectance ratio ρ can be expressed in terms of n_i, k_i (complex refractive index) and d_i (thickness)

-> n_i and k_i are functions of the wavelength

-> dispersion laws are mathematical functions modelling the optical properties of a material (e.g. *Cauchy's equation*)

$$n(\lambda) = A + \frac{B}{\lambda^2} + \frac{C}{\lambda^4} \qquad k(\lambda) = D + \frac{E}{\lambda^2} + \frac{F}{\lambda^4}$$

Cauchy's equation

-> ellipsometry software usually also provides a database with optical properties for a wide range of materials

Post-Polymerization Modification of PGMA Brushes

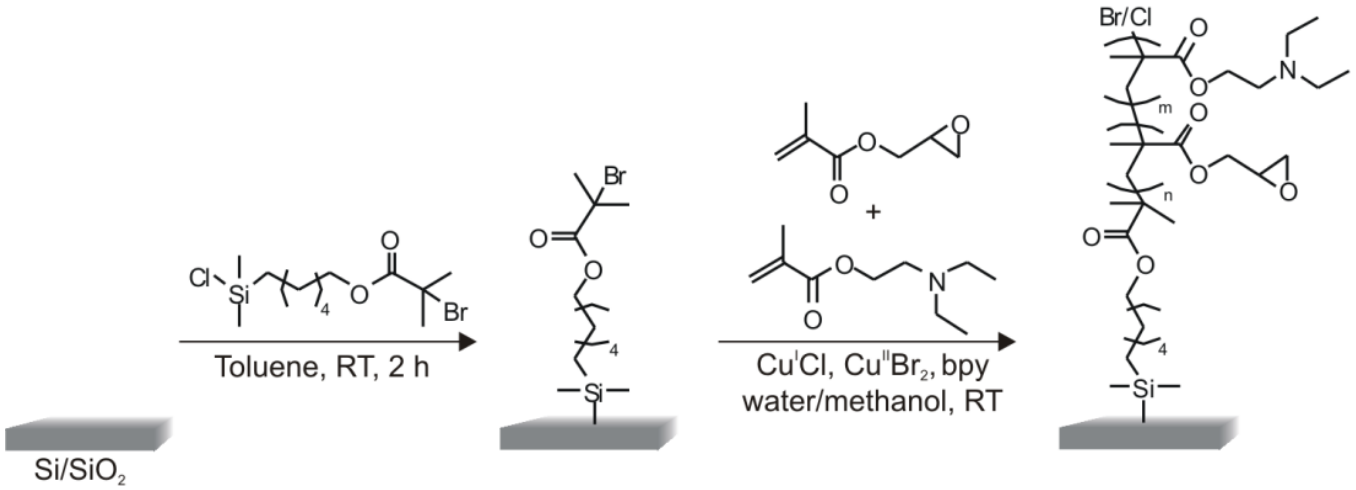

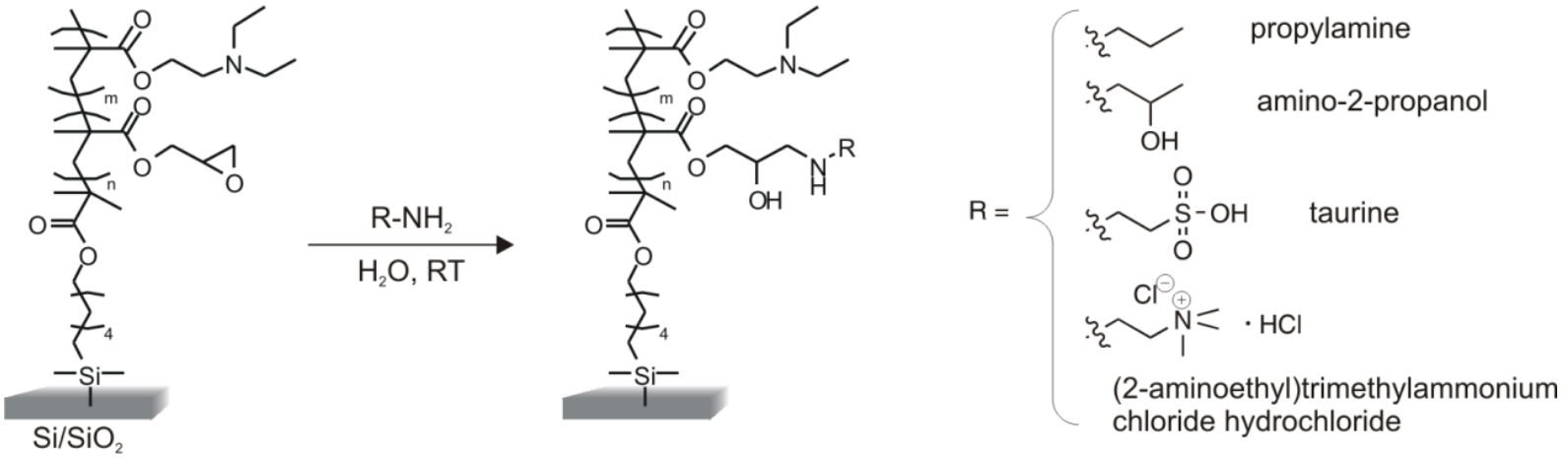

R. Barbey, H.-A. Klok, *Langmuir* **2010**, *26*, 18219

Surface-Initiated Polymerization

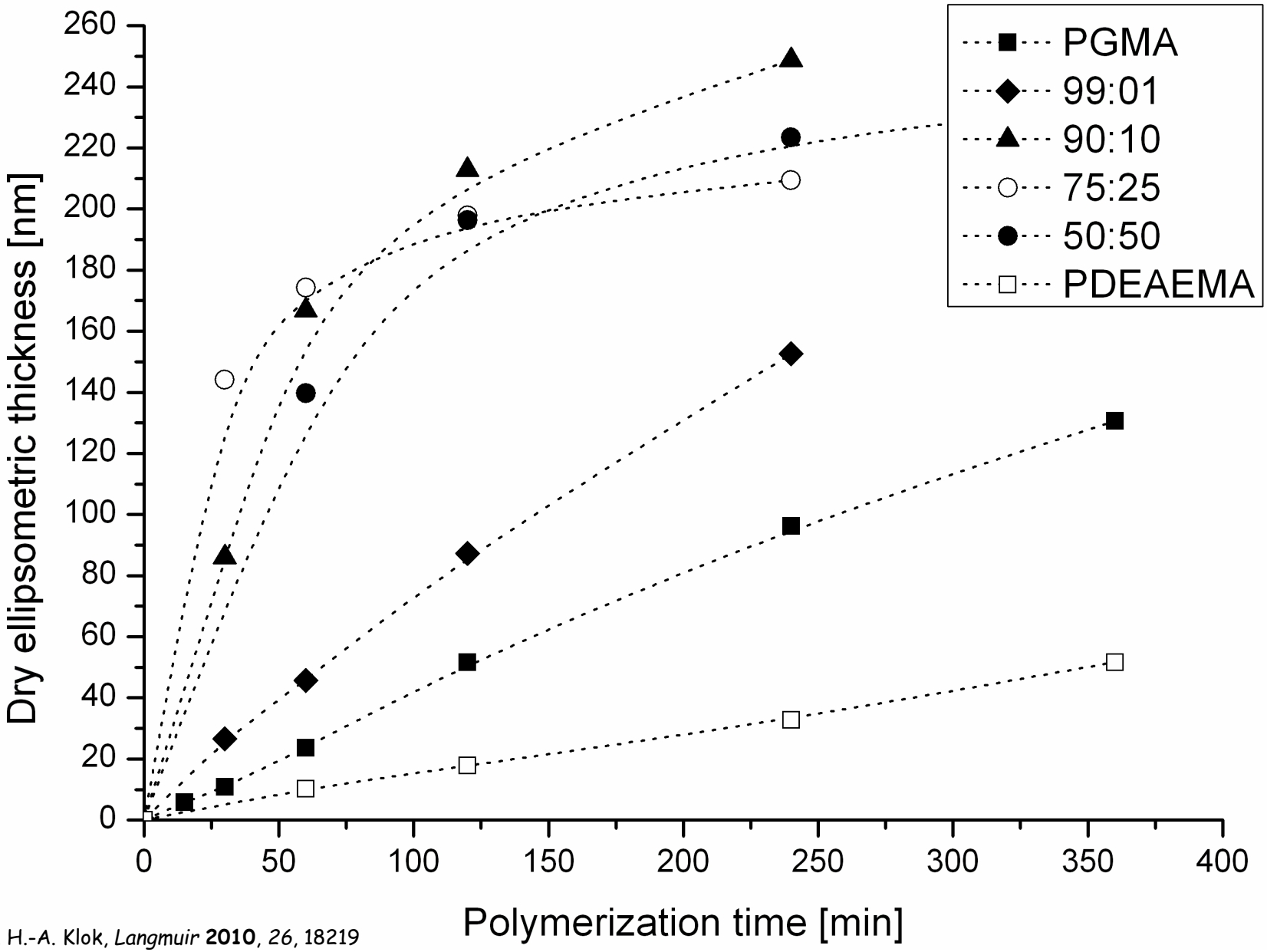

R. Barbey, H.-A. Klok, *Langmuir* **2010**, *26*, 18219

Determining M_n and Grafting Density

Surface-Cleavage of Polymer Brushes and Solution Characterization

- mostly using HF or TBAF
- works well from nanoparticles
- for planar surface, sufficiently large surface area is needed
- cleaved polymer can be analyzed using standard polymer characterization, e.g. GPC

Langmuir

Article

pubs.acs.org/Langmuir

On-Demand Degrafting and the Study of Molecular Weight and Grafting Density of Poly(methyl methacrylate) Brushes on Flat Silica Substrates

Rohan R. Patil,[†] Salomon Turgman-Cohen,[‡] Jiří Šrogl,[†] Douglas Kiserow,[†,§] and Jan Genzer*[,†]

[†]Department of Chemical and Biomolecular Engineering, North Carolina State University, Raleigh, North Carolina 27695-7905, United States

[‡]Department of Chemical Engineering, Kettering University, Flint, Michigan 48504, United States

[§]US Army Research Office, Research Triangle Park, North Carolina 27709-2211, United States

Supporting Information

ABSTRACT: We report on degrafting of surface-anchored poly(methyl methacrylate) (PMMA) brushes from flat silica-based substrates using tetrabutylammonium fluoride (TBAF) and determining their molecular weight distribution (MWD) using size exclusion chromatography (SEC). The grafted PMMA layer was synthesized using surface-initiated atom transfer radical polymerization (SI-ATRP) of MMA for polymerization times ranging from 6 to 24 h. X-ray photoelectron spectroscopy, ellipsometry, and time-of-flight secondary ion mass spectrometry were employed in tandem to characterize the degrafting process. The SEC eluograms were fit to various polymer distributions, namely Zimm−Schulz, ATRP in continuous stirred tank reactor, Wesslau, Schulz−Flory, and Smith et al. The ATRP model gives the best fit to the experimental data. The dry PMMA brush thickness and the number-average molecular weight (obtained from the MWD) suggest that the grafting density of the PMMA grafts is independent of polymerization time, indicating well-controlled/living growth of MMA. The observed polydispersity index (PDI) was higher than that generally observed in bulk grown polymers under similar conditions, indicating an effect due to chain confinement and crowding. We detect small but noticeable dependence of the polymer brush grafting density on the inhibitor/catalyst ratio. Higher inhibitor/catalyst ratio offers better control with lower early terminations, which results in a small increase in the apparent grafting density of the chains.

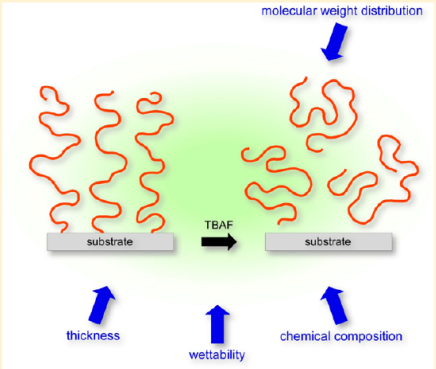

R. R. Patil, S. Turgman-Cohen, J. Srogl, D. Kiserow, J. Genzer, *Langmuir* **2015**, *31*, 2372-2381

Solution Characterization of Cleaved PMMA

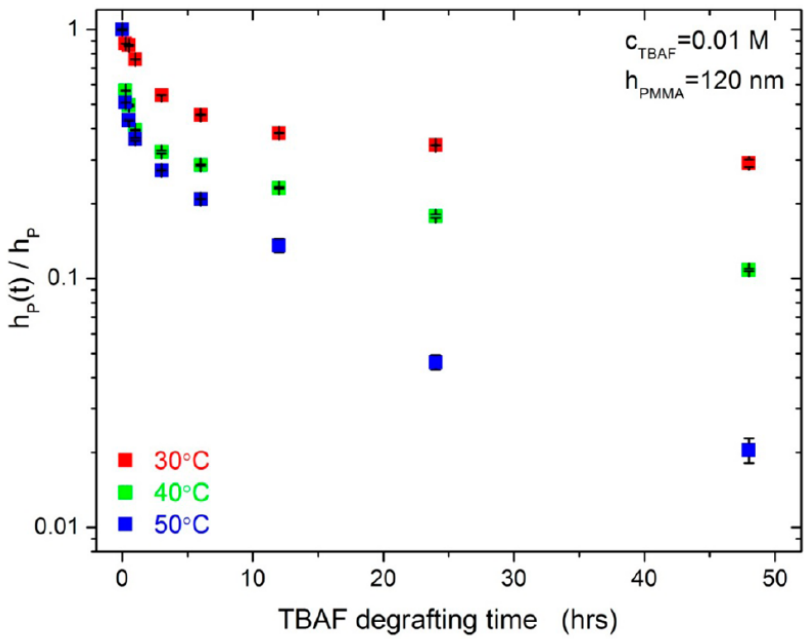

Figure 4. Relative brush thickness (i.e., time-dependent thickness normalized by the initial thickness) of a PMMA brush as a function of TBAF degrafting time at three different temperatures. The original dry thickness of the PMMA brush was ~120 nm, and the concentration of the TBAF solution was 0.01 M.

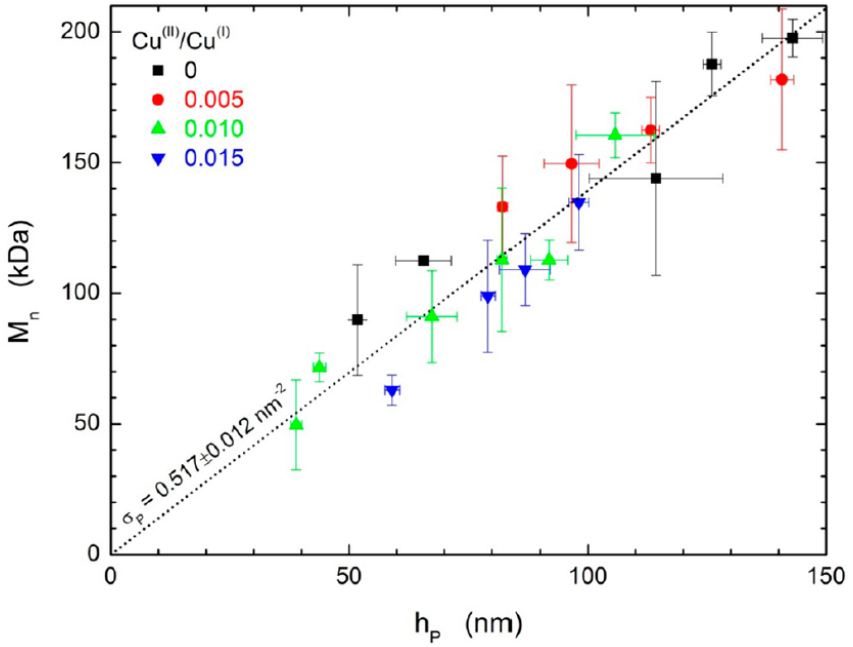

Figure 8. Number-average molecular weight (M_n) as a function of dry PMMA brush thickness (h_p) for four ATRP catalyst ratios. The dotted line is a linear fit passing through the origin.

Note: $M_n = \frac{h \rho NA}{\sigma}$

R. R. Patil, S. Turgman-Cohen, J. Srogl, D. Kiserow, J. Genzer, *Langmuir* **2015**, *31*, 2372-2381

Sacrificial Initiator – Fact or Fiction ?

- Sometimes a **sacrificial initiator** (e.g. ethyl 2-bromoisobutyrate) is added to the reaction mixture for the growth of polymer brushes via SI-ATRP.
- Does analysis of the polymer generated by the sacrificial initiator provide insight into the molecular weight of the polymer grafts ?

Table 6. Overview of Polymer Brushes that Have Been Cleaved from Silicon Oxide Substrates Using Hydrofluoric Acid (HF) and Their Molecular Characteristics

Polymer Brush	Substrate Geometry	Cleaved Polymer Brush[a]			Free Polymer[b]		SI-CRP Technique
		M_n (kDa)	M_w/M_n	Grafting density (σ) (chains/nm^2)	M_n (kDa)	M_w/M_n	
Methacrylates							
PBMA	Nanoparticles	2300	1.16	-	-	-	AGET ATRP[308]
PBzMA	Nanoparticles	~48	~1.4	0.47	~48	~1.4	ATRP[1194]
PHEMA	Nanoparticles	9.3	1.12	-	-	-	ATRP[705]
PHPMAM	Mesoporous	11.5	1.28	-	-	-	RAFT[195]
PMAA	Nanoparticles	41	1.11	0.65	-	-	RAFT[209]
PMPC	Nanoparticles	20.9	1.72	0.066	-	-	ATRP[2038]
PPEGMA	Nanoparticles	125.4	1.32	0.79	-	-	ATRP[1129]
PTMSPMA	Nanoparticles	24.86	1.31	0.16	-	-	ATRP[1949]
PSBMA	Nanoparticles	71.2	1.48	0.20	-	-	ATRP[1266]
		68.9	1.90	0.32	-	-	ATRP[2057]
		206	1.21	0.071	-	-	ATRP[2060]
		23.8	1.27	0.129	-	-	ATRP[2038]
	Planar	176	1.80	0.080	365	1.74	ATRP[329]
PDMAEMA	Nanoparticles	79.9	1.38	0.26	-	-	ATRP[1266]
		98.7	3.11	0.14	-	-	ATRP[679]
		36.15	1.14	0.077	-	-	ATRP[1073]
PDEAEMA	Mesoporous	23.6	1.14	-	-	-	ATRP[1211]
PMMA	Nanoparticles	17	1.31	-	21.3	1.34	ATRP[1679]
		9.69	1.18	-	-	-	ATRP[814]
		62	2.5	0.10	-	-	ATRP[236]
		105.1	~1.5	0.37	~65	~1.4	AGET ATRP[338]
		222	1.51	0.93	228	1.54	ARGET ATRP[1737]
		191	~1.27	0.5	~205	~1.28	ATRP[246]
		48.7	1.47	0.36	90.8	1.60	RAFT[204]
		~510	~1.2	0.45	~480	~1.3	ATRP[466]
		17.89	1.2	-	-	-	ATRP[302]
		410	1.20	-	-	-	AGET ATRP[308]
		27000	1.17	-	-	-	AGET ATRP[308]
		40.2	1.34	-	-	-	ATRP[327]
		62.4	1.47	0.54	-	-	AGET ATRP[1739]
		205	<1.3	0.07	-	-	RAFT[208]
		108	1.24	-	-	-	ATRP[1571]
	Mesoporous	54.22	1.6	0.05	-	-	ATRP[302]
		43.72	1.4	0.05	63.73	1.12	ATRP[302]
Acrylates							
P*t*BA	Nanoparticles	24.2	1.09	0.20	21.0	1.10	RAFT[187]
PBBEA	Mesoporous	29.2	1.80	-	-	-	ATRP[1319]
PAPBA-PA	Porous beads	-	-	-	-	-	ATRP[2133]
PMA	Nanoparticles	2400	1.18	-	-	-	AGET ATRP[308]
PMA (loops)	Nanoparticles	53 (M_p)	2.0	-	~100 (M_p)	-	RAFT[206]
		31 (M_p)	-	-	80 (M_p)	-	RAFT[207]
PCPPUA	Porous beads	3.85	1.15	-	-	-	ATRP[1130]
PBA	Nanoparticles	79.4	1.29	-	-	-	AGET ATRP[1087]
		100	1.07	0.31	105	1.24	RAFT[204]

J. Zoppe, N. Cavusoglu Ataman, P. Mocny, J. Wang, J. Moraes, H.-A. Klok, *Chem. Rev.* **2017**, *117*, 1105

Sacrificial Initiator – Fact or Fiction ?

		205	<1.3	0.07	-	-	RAFT[208]
		108	1.24	-	-	-	ATRP[1571]
	Mesoporous	54.22	1.6	0.05	-	-	ATRP[302]
		43.72	1.4	0.05	63.73	1.12	ATRP[302]
Acrylates							
P*t*BA	Nanoparticles	24.2	1.09	0.20	21.0	1.10	RAFT[187]
PBBEA	Mesoporous	29.2	1.80	-	-	-	ATRP[1319]
PAPBA-PA	Porous beads	-	-	-	-	-	ATRP[2133]
PMA	Nanoparticles	2400	1.18	-	-	-	AGET ATRP[308]
PMA (loops)	Nanoparticles	53 (M_p)	2.0	-	~100 (M_p)	-	RAFT[206]
		31 (M_p)	-	-	80 (M_p)	-	RAFT[207]
PCPPUA	Porous beads	3.85	1.15	-	-	-	ATRP[1130]
PBA	Nanoparticles	79.4	1.29	-	-	-	AGET ATRP[1087]
		100	1.07	0.31	105	1.24	RAFT[204]
Acrylamides							
PNIPAM	Nanoparticles	113	1.33	0.31	106	1.33	RAFT[204]
		64	1.25	0.55	-	-	ATRP[817]
		7.4	1.19	0.36	7.2	1.19	ATRP[1061]
	Mesoporous	2.8	~1.26	-	-	-	ARGET ATRP[1306]
	Porous beads	13.3	3.13	0.125	-	-	ATRP[2395]
	Monoliths	9.7	2.23	0.072	-	-	ATRP[2395]
	Planar	42.3	1.11	1.2	44	1.13	ATRP[337]
Styrenic							
PS	Nanoparticles	17.2	1.17	-	18	1.21	ATRP[1679]
		9.1	1.09	-	-	-	ATRP[2496]
		~220	1.3	0.2	~130	1.6	RAFT[204]
		88.8	1.37	0.2	-	-	ATRP[237]
		20	1.27	0.24	-	-	ATRP[307]
		7.58	1.22	-	-	-	ATRP[816]
		12.7	1.25	-	-	-	RAFT[210]
		96.9	1.10	-	-	-	ATRP[311]
		119	<1.3	0.047	-	-	RAFT[208]
		80.4	1.32	0.5	-	-	ARGET ATRP[1080,2492]
		203	~1.2	0.55	-	-	ATRP[342]
	Mesoporous	24.8	2.1	0.2	24.5	1.22	NMP[467]
		3.27	9.7	-	18.92	1.15	ATRP[302]
	Planar hole array	~72	~1.32	-	-	-	ATRP[555]
PSS(Na)	Nanoparticles	23.8	1.7	-	-	-	ATRP[1144]

J. Zoppe, N. Cavusoglu Ataman, P. Mocny, J. Wang, J. Moraes, H.-A. Klok, *Chem. Rev.* **2017**, *117*, 1105

Sacrificial Initiator – Fact or Fiction ?

Table 7. Overview of Polymer Brushes that Have Been Cleaved from Silicon Oxide Substrates Using Reagents Other than Hydrofluoric Acid (HF) and Their Molecular Characteristics

Polymer Brush	Substrate Geometry	Cleaving Agent	Cleaved Polymer Brush[a]			Free Polymer[b]		SI- CRP Technique
			M_n (kDa)	M_w/M_n	Grafting density (σ) (chains/nm^2)	M_n (kDa)	M_w/M_n	
Methacrylates								
PLMA	Planar	UV	900	2.0	0.13	-	-	ATRP[244]
PMETAC	Planar	H_2SO_4	101	1.29	0.20	130	1.15	ATRP[251]
PMMA	Planar	tetrabutyl ammonium fluoride (TBAF)	200	1.15	0.52	-	-	ATRP[842]
PDMAEMA	Nanoparticles	*p*-toluenesulfonic acid	17.8	1.12	-	-	-	ATRP[247]
PTMSPMA	Nanoparticles		7.9	1.14	0.20	-	-	ATRP[248]
Acrylates								
PAA	Planar	Tris(hydroxymethyl) aminomethane buffer	-	-	-	-	-	ATRP[252]
PMA	Nanoparticles	AIBN	~12.5	~1.6	-	~21	~1.3	RAFT[205]
Acrylamides								
PNIPAM	Planar	NaOH	~6.3	-	-	-	-	ATRP[2382]
	Porous beads		18.9	2.69	0.133	-	-	ATRP[2393]
			16.1	2.94	0.106	-	-	ATRP[2396]
PNTBAM	Porous beads		4.7	1.77	0.080	-	-	ATRP[2396]
Styrenic								
PS	Planar	UV	70	1.9	0.44	-	-	ATRP[244]
		p-toluenesulfonic acid	37.3	1.26	0.83	26.6	1.28	ATRP[240]
	Mesoporous	-	240.8	1.30	-	-	-	SET/SARA[98]
	Nanoparticles	-	156.9	1.29	-	-	-	SET/SARA[98]
		p-toluenesulfonic acid	16.1	1.13	-	19.1	1.35	ATRP[249]
Block copolymers								
PMMA-*b*-PMDPAB	Planar	Ammonium bifluoride (NH_4HF_2)	140	1.22	-	130	-	ATRP[253]
PMA-*b*-PS	Nanoparticles	AIBN	21.4	1.42	-	18.7	1.53	RAFT[205]
PTMSPMA-*b*-PHFBMA	Nanoparticles	*p*-toluenesulfonic acid	26.8	1.27	0.20	-	-	ATRP[248,250]
PS-*b*-PTMSPMA	Nanoparticles		41.1	1.24	-	-	-	ATRP[249]
Random copolymers								
PPEGMA-*co*-PPEGMEMA	Nanoparticles	NaOH	165.8	1.28	-	-	-	ATRP[509]
PNIPAM-*co*-PAPTAC-*co*-PNTBAM	Porous beads		15.8	1.67	0.09	5.1	1.27	ATRP[2318]
PNIPAM-*co*-PMBAM	Porous beads		9.1	2.68	0.021	-	-	ATRP[2396]
PNIPAM-*co*-PNTBAM	Porous beads		18.6	1.89	0.067	-	-	ATRP[2396]
PNIPAM-*co*-PDMAEMA-*co*-PNTBAM	Monoliths		12.9	2.53	0.072	-	-	ATRP[1321]
	Porous beads		17.4	3.13	0.11	-	-	ATRP[1321]
PNIPAM-*co*-PAA-*co*-PNTBAM	Monoliths		13.8	1.48	0.169	-	-	ATRP[626]
	Porous beads		12.1	1.53	0.131	-	-	ATRP[626]

[a]Results refer to values corresponding to the highest number-average molecular weight (M_n) obtained by the cited authors for cleaved polymer brushes. [b]Bulk or solution polymers produced simultaneously or under the same reaction conditions. The superscripts are references to the relevant publications.

J. Zoppe, N. Cavusoglu Ataman, P. Mocny, J. Wang, J. Moraes, H.-A. Klok, *Chem. Rev.* **2017**, *117*, 1105

Determining M_n and Grafting Density

Direct characterization of molar mass and grafting density

- No brush cleavage needed
- Techniques:
  - Single molecule atomic force microscopy
  - Analysis of swollen polymer films thicknesses

Single-Molecule Atomic Force Microscopy

J. Phys. Chem. B **2001,** *105,* 3965−3971

Study of the Polydispersity of Grafted Poly(dimethylsiloxane) Surfaces Using Single-Molecule Atomic Force Microscopy†

Sabah Al-Maawali, Jason E. Bemis, Boris B. Akhremitchev, Rojana Leecharoen, Benjamin G. Janesko, and Gilbert C. Walker*

Department of Chemistry, University of Pittsburgh, Pittsburgh, Pennsylvania 15260

Received: October 10, 2000; In Final Form: November 29, 2000

Single-molecule atomic force microscopy (AFM) was used to study the statistical distribution of contour lengths (polydispersity) of polymer chains grafted to a surface. A poly(dimethylsiloxane) (PDMS) monolayer was grafted on a flat silicon substrate by covalently bonding Cl-terminated PDMS (M_w = 15000−20000) to an OH−silicon surface and characterized using contact angle measurements, ellipsometry, and single-molecule AFM. A model for the single-chain dynamics is presented. The statistical distributions of the polymer contour lengths were found to depend on the concentration of the PDMS polymer used in the grafting solutions. Shifts of the statistical distributions toward higher contour lengths indicated preferential adsorption of longer chains with increasing PDMS:CH_2Cl_2 volume ratios of 0.005−0.16. The gel permeation chromatography (GPC) profile was found to correlate with the most dilute (0.005 volume ratio) AFM data. The polydispersity index (PI) calculated using AFM data was found to be 1.56 compared to 1.62 by GPC. A surface grafted with two PDMS polymer samples of average molecular weights, 3000 and 15000−20000, was found to have a bimodal distribution of contour lengths, with peaks corresponding to the two grafting samples.

Single-Molecule Atomic Force Microscopy

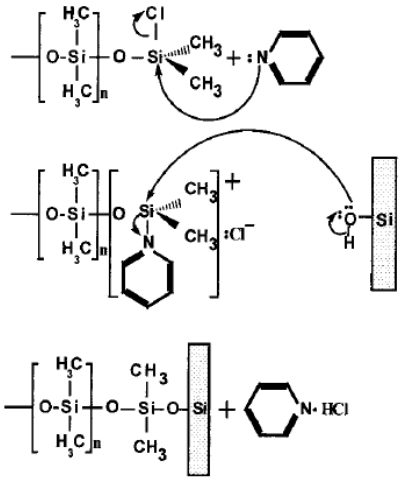

Figure 2. Mechanism for grafting Cl-terminated PDMS on a silicon surface.[21]

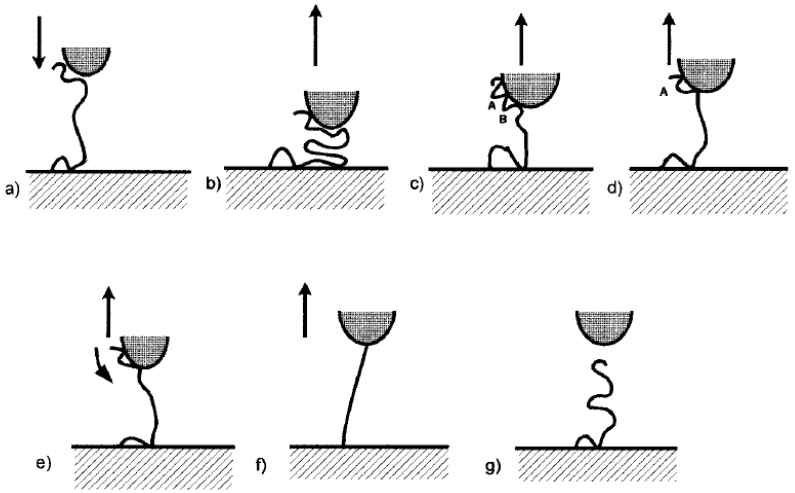

Figure 1. Stages of tip−polymer interaction. (a) Before interaction with the tip, the polymer, grafted to the surface at one end, is in a brush state, again with a small number of monomers on the surface which separate the adsorbed chain into a series of loops and a tail. (b, c) The AFM tip, when it comes into contact with the surface, also creates a collection of contacts with the polymer that lead to a distribution of loops and a tail. Other tip−surface contacts are also formed, whose release may be described by a well-known JKR contact mechanism,[22] and are illustrated here. (d, e) The process of separating the tip and surface creates a stress on the polymer chain. This stress is at first released by sliding the polymer chain along one of the surfaces. This causes monomer−surface contacts to collect. (f) At some point of tip separation from the surface, no more stress can be released by such sliding or snakelike motion, and significant stretching of the chain occurs. (g) Finally, complete rupture of the chain from the tip follows, with the sudden rupture of the collected monomer−surface contacts.

Single-Molecule Atomic Force Microscopy

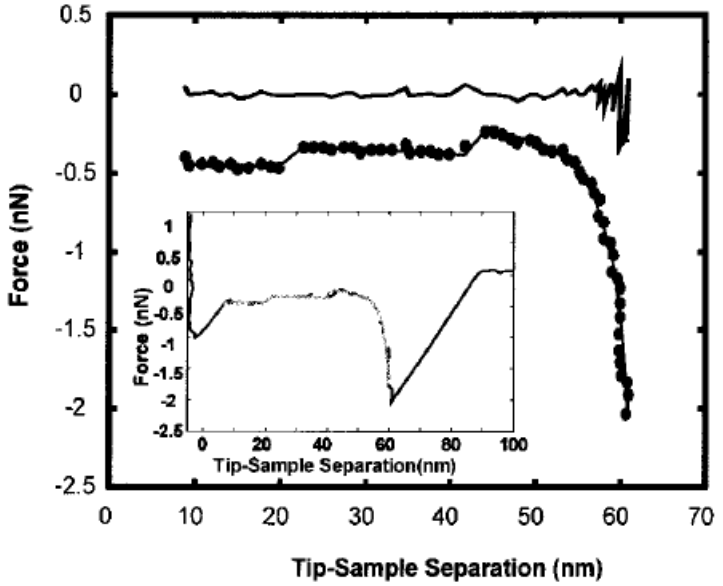

Figure 4. Force plot with a primary adhesion and a secondary adhesion due to PDMS stretching. The flat, steplike profile is caused by the chain sliding on the tip, as described in the text. The persistence length obtained from fitting the hybrid model is 0.13 nm, suggesting that, unlike in Figure 3, a loop is being stretched. The error between the data and the fitted values is indicated by the line above the fitted data. The inset shows the entire force plot.

Model for Nonlinear Extension of the Chain. The extension of the chain can cause non-Gaussian distributions of its end-to-end length. We calculate the forces required to generate such conformations using the wormlike chain (WLC) model. This model describes a polymer chain as consisting of N bonds with fixed lengths l joined in a linear succession. The WLC model maintains the angles at the bond junctions fixed, but the dihedral angles are free to rotate.[8,9,10a,12,32] The elastic restoring force of the polymer chain, F_{chain} (nN), is calculated as follows:

$$F_{chain} = \frac{k_B T}{p}\left(\frac{1}{4(1 - r/L_{contour})^2} - \frac{1}{4} + \frac{r}{L_{contour}}\right) \qquad (2)$$

where r (nm) is the end-to-end distance of the polymer chain, k_B is the Boltzmann constant, T is the temperature, p is the persistence length (nm), and $L_{contour}$ is the contour length (nm) of the polymer chain.

Single-Molecule Atomic Force Microscopy

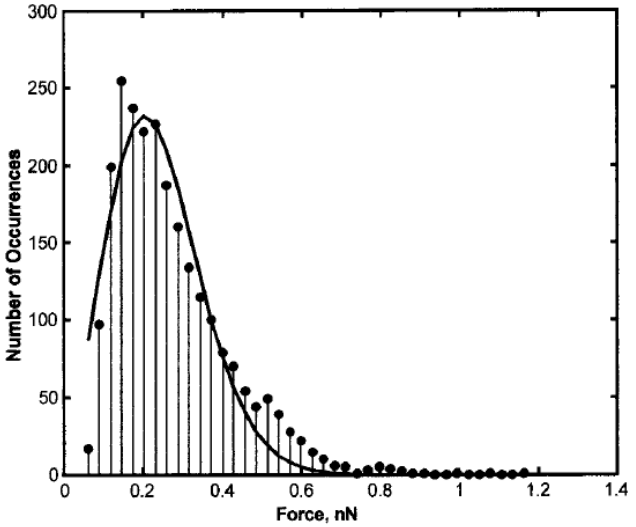

Figure 5. Statistical distribution of polymer stretching rupture forces observed between the AFM tip and the PDMS monolayer at the surface.

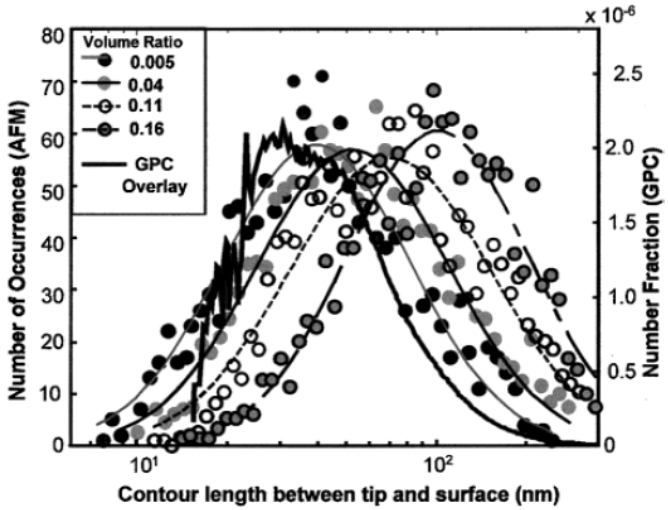

Figure 6. GPC profile overlaid with the AFM statistical distributions of contour length between the tip and surface for different PDMS: CH_2Cl_2 volume ratios indicated in the plot. See the text for further explanation.

Using AFM results of contour lengths (L_i), we convert them to molecular weights using the following equation:

$$M_i = \frac{74 L_i}{0.28\ \text{nm}} \tag{3}$$

Here, 74 is the molecular weight of one siloxane monomer and 0.28 nm is the length of one monomer. Average M_n and M_w are calculated as follows:

$$\bar{M}_n = \frac{1}{N}\sum M_i \tag{4}$$

$$\bar{M}_w = \frac{\sum_i M_i^2}{\sum_i M_i} \tag{5}$$

Analysis of Swollen Polymer Brush Thicknesses

Alexander-de Gennes model

LE JOURNAL DE PHYSIQUE TOME 38, AOUT 1977, PAGE 983

Classification
Physics Abstracts
5.600 — 7.852

ADSORPTION OF CHAIN MOLECULES WITH A POLAR HEAD A SCALING DESCRIPTION

S. ALEXANDER (*)

Physique de la Matière Condensée,
Collège de France, 11, pl. Marcelin-Berthelot, 75231 Paris Cedex 05, France

(*Reçu le 24 mars 1977, accepté le 4 mai 1977*)

Résumé. — L'adsorption de molécules en chaînes à une interface est étudiée en supposant que chaque molécule présente un point d'interaction localisé sur la chaîne (du type tête polaire) et une interaction uniforme de ses monomères avec la surface. Une description en terme de lois d'échelles des configurations de chaînes et des interactions est discutée. L'existence d'une attraction de surface uniforme affecte profondément le diagramme de phase. Un régime bidimensionnel de faible densité et une phase haute densité avec les chaînes confinées dans des cylindres étroits peuvent être rencontrés. La transition entre les deux phases est du premier ordre. Les lois de puissance pour la densité à l'interface, l'épaisseur de la couche et la pression de surface sont dérivées. Le comportement des lipides et agents de surface à chaînes courtes est qualitativement semblable et il est suggéré qu'une interaction de surface uniforme peut aussi jouer un rôle important dans ce cas.

Abstract. — The adsorption of chain molecules at an interface is investigated assuming that the molecule has both a polar head type of attraction localized on the chain and a uniform interaction of the chain monomers with the surface.

A scaling description of the chain configurations and interactions is used. It is shown that the presence of a uniform surface attraction changes the phase diagram drastically. Both a low density two-dimensional regime and a high density phase with the chains confined in narrow cylinders can occur. The transition between the two phases is first order. Power laws for the surface density, layer thickness and surface pressure are derived. The qualitative similarity with the behaviour observed for short chain lipids and surfactants is also noted and it is suggested that a uniform surface interaction may also play an important role there.

Macromolecules **1980**, *13*, 1069–1075 **1069**

Conformations of Polymers Attached to an Interface

P. G. de Gennes

Collège de France, 75231 Paris Cedex 05, France. *Received April 10, 1980*

ABSTRACT: We discuss the conformations and the concentration profiles for long, flexible chains (N monomers per chain) grafted at one end on a solid surface (fraction of surface sites grafted σ). The chains are immersed either in a pure (good) solvent or in a solution of the same polymer (P monomers per mobile chain, volume fraction ϕ). It is assumed that the polymer does *not* adsorb on the wall surface. The zone occupied by the grafted chain may contain a large fraction of mobile P chains: we call this a mixed case (M), as opposed to the unmixed case (UM). Also the chains may be stretched (S) or unstretched (US). The combination of these two criteria gives four possible regimes. Using scaling laws, we locate the domains of existence of these four regimes in terms of the variables σ and ϕ. High σ values may be hard to reach by grafting but could be obtained with block copolymers at an interface between two immiscible solvents.

Analysis of Swollen Polymer Brush Thicknesses

Alexander-de Gennes model

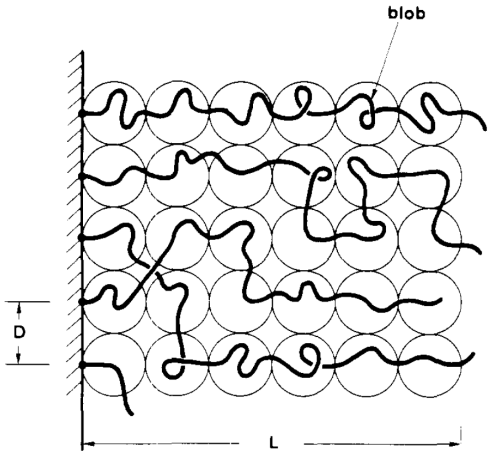

Figure 5. Strongly stretched situation for a grafted layer in good solvent. The chains are mainly stretched along the norm to the wall.

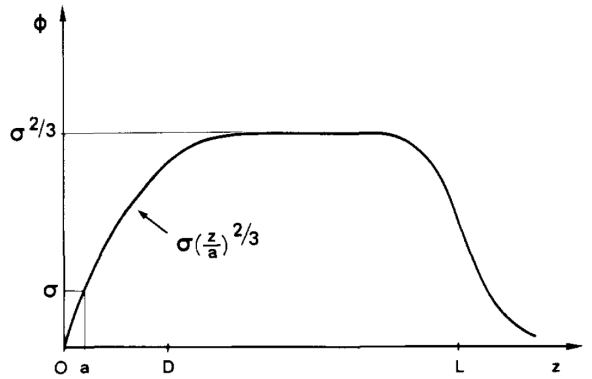

Figure 6. Concentration profile for a grafted layer immersed in a good solvent in the overlapping regime.

P.G. de Gennes, *Macromolecules* **1980**, *13*, 1069-1075

$$\sigma = a^{-2} \cdot \alpha^{\left(\frac{2n}{1-3n}\right)}$$

a = monomer size:
α = swelling ratio;
n = solvent quality
(*n* = 0.5 for θ-solvents)

$$\alpha = \frac{h_{swollen}}{h_{dry}}$$

$$\sigma = a^{-2} \cdot \left(\frac{h_{dry}}{h_{swollen}}\right)^2$$

in a θ-solvent

$h_{swollen}$ and h_{dry} can be obtained, for example, from ellipsometry or AFM

With h_{dry} and σ, M_n follows from:

$$\sigma = \frac{h\,\rho\,NA}{M_n}$$

Analysis of Swollen Polymer Brush Thicknesses

Milner-Witten-Cates Model

Macromolecules **1988**, *21*, 2610–2619

Theory of the Grafted Polymer Brush

S. T. Milner* and T. A. Witten

Corporate Research Science Laboratories, Exxon Research and Engineering Company, Annandale, New Jersey 08801

M. E. Cates

Institute for Theoretical Physics, University of California, Santa Barbara, California 93106.
Received October 5, 1987

ABSTRACT: We calculate the free energy of surfaces coated with grafted polymers in a solvent. We use a self-consistent field (SCF) method appropriate for weak excluded-volume interactions and at moderately high surface coverage. We give the exact solution for the "classical limit" of our SCF equations which shows that, at high molecular weight, the concentration profile approaches a parabolic form rather than the step-function suggested by Alexander and de Gennes. Accordingly, the energy required to slightly compress the brush varies as the cube of the compression distance. An extension of the method to the good-solvent, semidilute regime is described.

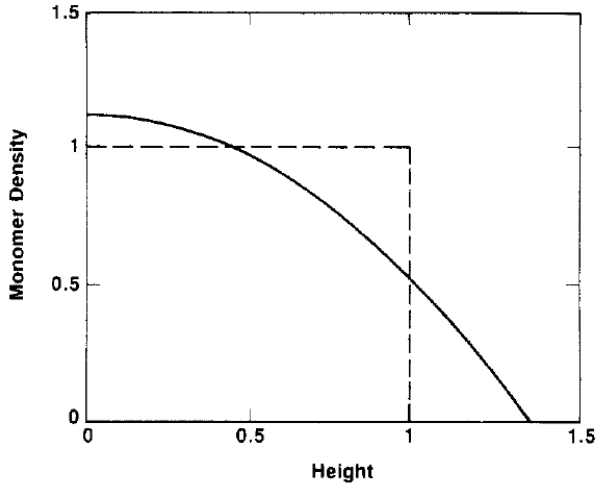

Figure 2. Density profiles $\phi(z)$ of the parabolic brush and the step-function Ansatz at equal coverage σ and molecular weight N.

Analysis of Swollen Polymer Brush Thicknesses

Milner-Witten-Cates Model

Milner-Cates model defines the degree of polymerization as

$$N = \left(\frac{\pi^2}{12}\frac{M_0}{\rho\, N_A}\frac{\upsilon}{\omega}\right)^{1/2} \cdot h_{swollen}^{3/2} \cdot h_{dry}^{-1/2}$$

where M_0 is the monomer molecular weight, ρ the bulk polymer density, $v = (3/a^2)$ with a as the Kuhn length, N_A Avogadro's number, and ω is the excluded volume parameter.

$h_{swollen}$ and h_{dry} can be obtained, for example, from ellipsometry or AFM

With h_{dry} and M_n, σ follows from: $$\sigma = \frac{h\,\rho\,NA}{M_n}$$

Analysis of Linear, Y- and Ψ-Shaped Brushes

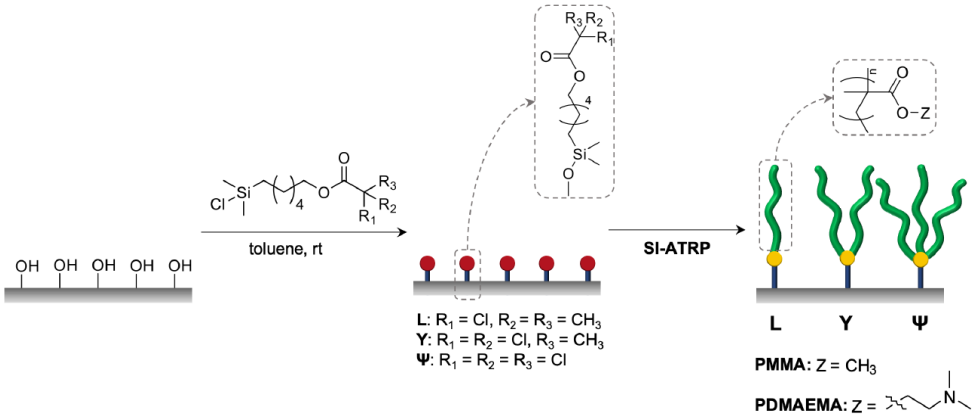

Scheme 1: Synthesis of L-, Y-, and Ψ-shaped PMMA and PDMAEMA brushes via atom transfer radical polymerization from a homologous series of surface-attached initiators.

Table 1: Swelling ratios (α) and grafting densities (σ) of linear, Y-, and Ψ-shaped PMMA and PDMAEMA brushes obtained using the box model to fit ellipsometric data of swollen polymer brushes and by applying the Alexander-deGennes model to determine grafting densities.

		h_{dry} [nm]	$h_{swollen}$ [nm]	α [-]	σ [chains/nm^2]
PMMA	**Linear**	54 ± 4	187 ± 2	3.4 ± 0.3	0.15 ± 0.02
	Y-shaped	54 ± 5	111 ± 6	2.1 ± 0.2	0.41 ± 0.08
	Ψ-shaped	52 ± 7	152 ± 13	3.0 ± 0.5	0.20 ± 0.06
PDMAEMA	**Linear**	48 ± 6	224 ± 14	4.7 ± 0.7	0.08 ± 0.02
	Y-shaped	52 ± 1	155 ± 6	3.0 ± 0.1	0.20 ± 0.02
	Ψ-shaped	34 ± 1	135 ±3.4	4.0 ± 0.2	0.11 ± 0.01

Table 2: Swelling ratios (α), number-average degree of polymerization (N) and grafting densities (σ) of linear, Y-, and Ψ-shaped PMMA and PDMAEMA brushes obtained using the gradient model to fit ellipsometric data of swollen polymer brushes, and by applying the Milner-Cates model to determine number-average degrees of polymerization (N) and grafting densities (σ).

		h_{dry} [nm]	$h_{swollen}$ [nm]	α [-]	N [-]	σ [chains/nm^2]
PMMA	**Linear**	54 ± 4	260 ± 2	4.8 ± 0.4	6098 ± 255	0.06 ± 0.01
	Y-shaped	54 ± 5	172 ± 10	3.2 ± 0.3	3301 ± 325	0.12 ± 0.02
	Ψ-shaped	52 ± 7	255 ± 31	5.0 ± 0.9	6102 ± 1176	0.06 ±0.02
PDMAEMA	**Linear**	48 ± 6	239 ± 17	5.0 ± 0.7	5734 ± 717	0.05 ± 0.01
	Y-shaped	52 ± 1	184 ± 5	3.5 ± 0.1	3691 ± 170	0.08 ± 0.01
	Ψ-shaped	34 ± 1	151 ± 2	4.5 ± 0.2	3430 ± 104	0.06 ± 0.01

S. Sant, H.-A Klok, unpublished data